



The proteome of neutrophils in sickle cell disease reveals an unexpected activation of interferon alpha signaling pathway

Patricia Hermand, Slim Azouzi, Emilie-Fleur Gautier, François Guillonnet, Vincent Bondet, Darragh Duffy, Sébastien Dechavanne, Pierre-Louis Tharaux, Patrick Mayeux, Caroline Le van Kim, et al.

► To cite this version:

Patricia Hermand, Slim Azouzi, Emilie-Fleur Gautier, François Guillonnet, Vincent Bondet, et al.. The proteome of neutrophils in sickle cell disease reveals an unexpected activation of interferon alpha signaling pathway. *Haematologica*, 2020, pp.haematol.2019.238295. 10.3324/haematol.2019.238295 . pasteur-02505633

HAL Id: pasteur-02505633

<https://pasteur.hal.science/pasteur-02505633>

Submitted on 11 Mar 2020

HAL is a multi-disciplinary open access archive for the deposit and dissemination of scientific research documents, whether they are published or not. The documents may come from teaching and research institutions in France or abroad, or from public or private research centers.

L'archive ouverte pluridisciplinaire **HAL**, est destinée au dépôt et à la diffusion de documents scientifiques de niveau recherche, publiés ou non, émanant des établissements d'enseignement et de recherche français ou étrangers, des laboratoires publics ou privés.



Distributed under a Creative Commons Attribution - NonCommercial 4.0 International License

The proteome of neutrophils in sickle cell disease reveals an unexpected activation of interferon alpha signaling pathway

Patricia Hermand^{1,2}, Slim Azouzi^{1,2}, Emilie-Fleur Gautier^{2,3}, François Guillonnet^{2,3}
Vincent Bondet⁴, Darragh Duffy⁴, Sebastien Dechavanne^{1,2}, Pierre-Louis Tharaux^{2,5}, Patrick
Mayeux^{2,3}, Caroline Le Van Kim^{1,2*} and Berengere Koehl^{1,2,6*}

¹Université de Paris, UMR_S1134, BIGR, Inserm, Institut National de la Transfusion Sanguine, F-75015 Paris, France ; ²Laboratoire d'Excellence GR-Ex; ³Université de Paris, UMR_S1016, UMR 8104, Plateforme de Protéomique (3P5), Institut Cochin, Inserm, CNRS, F-75014, Paris, France ; ⁴Immunobiology of Dendritic Cells, Institut Pasteur, Inserm UMR 1223, F-75015 Paris, France; Université de Paris, Paris Cardiovascular Centre, PARCC, INSERM, F-75015, Paris, France; ⁵Sickle Cell Disease Center, Hematology Unit, Hôpital Robert Debré, Assistance Publique – Hôpitaux de Paris, F-75019 Paris, France.

* C.L.V.K. and B.K. contributed equally to this work

C.L.V.K. and B.K. are co-corresponding authors

Running title: Neutrophils proteome in Sickle Cell Disease

Author correspondence

Dr Berengere KOEHL: UMR_S 1134, University of Paris. I.N.T.S. – 6, rue Alexandre Cabanel 75739 PARIS Cedex 15. Phone: +33 (0)1 44 49 30 46 – Fax: +33 (0)1 43 06 50 19 - E-mail: berengere.koehl@inserm.fr

Pr Caroline Le Van Kim: UMR_S 1134, University of Paris. I.N.T.S. – 6, rue Alexandre Cabanel 75739 PARIS Cedex 15. Phone: +33 (0)1 44 49 30 46 – Fax: +33 (0)1 43 06 50 19 - E-mail: caroline.le-van-kim@inserm.fr

Polymorphonuclear neutrophils (PMNs) are key actors in the pathophysiology of sickle cell disease (SCD), but signaling pathways underlying their activation and sustained inflammation are not well documented. We thus investigated the protein profile of neutrophils from SCD patients (SS genotype) using proteomic approach. Unexpectedly, SCD neutrophils exhibit a high expression of Interferon Signaling Proteins (ISPs) belonging to the type 1 interferon (IFN-1) response pathway. We also showed that SCD patients at steady state displayed a higher level of plasmatic IFN α . Overall, we reported a dramatic high-level expression of ISPs in neutrophils from SS patients suggesting an abnormal activation that could be important in developing new anti-inflammatory therapies.

SCD is a hemoglobinopathy leading to major red blood cell (RBC) dysfunction, but other cell types (vascular endothelium, leukocytes, platelets) (1-3) also represent key actors in the pathophysiology of the disease. Important studies have highlighted the role of PMNs, both during the vaso-occlusive crisis (VOC) and the associated long-term morbidity and mortality (4). In SCD, patients have an increased leukocyte count at steady state, and exhibit neutrophil activation, rendering them more susceptible to inflammatory stimuli (5). Moreover recent data have demonstrated the presence of different sub-phenotypes of PMN especially in cancer and inflammation (6, 7) as well as in a preclinical model of SCD (8). Despite these advances, signaling pathways underlying sustained inflammation in SCD remain elusive. In addition, a fine understanding of PMN activation profile is necessary to better decipher the inflammatory paradigm in SCD and develop tailored therapies. In the present study, we investigated for the first time the proteomic profile of PMNs in SCD at basal state by a label-free global proteomic approach.

We performed a proteomic comparative study of purified neutrophils from 4 SS patients (SS1-4) at basal state and 4 AA healthy donors (AA1-4). All patients included in this study were homozygous (SS genotype), aged 2 to 18 years (mean age 9.7 years), and without any

associated co-morbidity. They were free from any infection and exhibited C-reactive protein level < 10 mg/l at the day of the inclusion. The controls were voluntary blood donors, all healthy and of AA genotype.

After mass spectrometry analysis, 4,634 proteins were identified and 4,487 of them could be reliably quantified. Restricting the analysis to proteins quantified in at least 75% of the samples and in at least one group (AA and/or SS) led to the comparison of 3,069 proteins (Figure 1A). To identify biological pathways modified in neutrophils from SS patients, we first performed a 2D annotation enrichment test (9) using GO, KEGG and Keywords annotation databases. This analysis revealed the presence of many neutrophil membrane and secreted proteins involved in immune response (Figure 1B). Next, we analyzed the SS and the AA proteomes and found 101 proteins significantly differentially expressed using a SS/AA ratio > 1.3 or < 0.7. Sixty-eight proteins were overexpressed (Cluster 1, Figure 1C), and 33 proteins were down-regulated in the SS group compared to the AA group (Cluster 2, Figure 1C). Before further investigate new biological pathway, we aimed to confirm the already known surface markers of sickle cell neutrophils. Indeed, several studies in mouse models or in patients have shown an activated and aged phenotype of PMNs in SCD (8, 10). By using our proteomics data, we found two proteins described as markers of activation (Fc fragment of IgG, high affinity Ia, receptor/CD64) and ageing (L-Selectin/ CD62L) of neutrophils respectively overexpressed (5.8 fold) and underexpressed (0.6 fold) in SS patients compared to the AA group (Supplementary Table 1 and proteomic file). These data were confirmed by cytometry analysis of freshly isolated neutrophils from 5 SS patients and 5 controls (Figure 1E). We therefore concluded that the proteomic analysis could be a relevant tool for exploring neutrophil abnormalities in SCD.

A Fisher exact test performed using proteins down-regulated in SS neutrophils did not evidence any common biological pathway (data not shown). In contrast, analyses of the

upregulated proteins revealed a major involvement of the type1 interferon (IFN-I) response (Supplementary Table 1 and proteomic file). Importantly, major ISPs including IFIT1, IFIT2, IFIT3, ISG15, ISG20, GBP2, IFI35, MX1 and MX2 were increased 3- to 84-fold in the proteome of SS neutrophils compared to the one of AA neutrophils (Figure 1D). Moreover, we found a significant overexpression of STAT1 and STAT2 in the neutrophil proteome of the SS group consistent with an activation of the IFN-related JAK/STAT signaling pathways. In order to confirm the proteomic data, we assessed the overexpression of the main ISPs using Western Blot experiments of purified neutrophils from 10 other SS patients at steady state and 10 other AA controls. In agreement with proteomic data, we found a significant increase of ISP expression including MX1, ISG15 and IFIT1 as well as the STAT1 and STAT2 proteins, in neutrophil lysates from SS patients compared to controls (Figure 2A). The nuclear translocation of STAT1 and STAT2 are activated by JAK and TYK2-mediated phosphorylation of the Y701 and Y689, respectively, that stimulates the IFN-I responses (11, 12). We showed that both Y701 of STAT1 and Y689 of STAT2 were highly phosphorylated in SS compared to AA neutrophils (Figure 2A). These findings confirmed the strong activation of the IFN-I signaling pathway in SS neutrophils via the JAK/STAT1/2 pathway.

To go further on and to assess whether the IFN-I response was due to either IFN α or IFN β , we measured the level of both cytokines in the plasma of 34 healthy AA donors and 37 SS patients at steady state, using the novel digital-ELISA technology. Interestingly, we found a significant increased level of IFN α in plasma from half of the SS patients compared to AA controls (Mann-Whitney test, $p < 0.001$), although no difference was observed for IFN β (Figure 2B). Although the specific role of the different types of IFN-I is not fully understood, it appears that IFN α , in contrast to IFN β is mainly involved in autoimmune and auto-inflammatory diseases (13). It is noteworthy that 20 SS patients exhibited an increase of IFN α from 10 to 1,000-fold compare to healthy individuals although 17 out of the 37 plasma

samples had normal levels of IFN α . Clinical and biological investigations of these 37 SS patients did not find any correlation between plasmatic level of IFN α and biologic markers including leucocyte, neutrophils, reticulocytes and platelets counts, Hemoglobin (Hb) level, Hb haplotypes or age (Supplementary Table 2), and plasmatic cytokine concentration (including CX3CL-1, Rantes, MCP-1, MCP-3, TNF α , IL1b, IL10, IL18, and IL6). Since it is known that neutrophil extracellular trap formation (NETosis) plays a role in the pathogenesis of SCD, we next investigated the NETosis by measuring the Neutrophil Elastase and nucleosome, in the plasma from 28 patients investigated for IFN α and IFN β . As expected, we found a significant high level of both markers of NETosis (Figure 2C) in SS patients compared to AA controls, but no correlation with the IFN α level (data not shown).

Finally, we analysed the clinical data from the patients, and found no significant difference between the “high IFN” and “low IFN” group of patients and the number of acute events (including number of VOC per year, acute chest syndrome, stroke, cerebral vasculopathy, acute splenic sequestration nor splenectomy). It is noteworthy that no patient has been treated with hydroxycarbamide and none of them followed a transfusion program.

Moreover, it is interesting to note that of the four SS plasma samples used for the neutrophil proteomic analysis one had low IFN α level, while the other three exhibited 7 to 60-fold increased levels compared to controls, although all the four neutrophil samples expressed high level of ISPs. Therefore, it is highly probable that plasma IFN α has a transient secretion while the downstream activation of the signaling pathway is persistent. Altogether, our data indicated that SS patients may have inappropriate transient high IFN α secretions (i.e., outside of any acute and infectious events), responsible for the activation of the IFN-1 signaling pathway in neutrophils. Although the mechanism of this activation remains to be elucidated, some recent data described a clear relationship between INF-1 responses and red blood cell alloimmunization in murine models (14, 15). Since alloimmunization represents a detrimental

issue in SCD, our data highlight the importance of testing the link between ISPs and alloimmunization in SS patients.

In conclusion, we showed for the first time by quantitative proteomic analyses of purified neutrophils a particular immune and inflammatory signature in SCD. Our findings provide evidence of a dysfunction of the IFN α signaling pathway that could play important role in the pathogenesis of SCD. Future studies using cohort of patients are needed to determine the relationship between IFN α activation and clinical complications and to establish if ISPs may represent therapeutic targets to decrease inflammation in SCD.

Acknowledgments

We thank the patients and their families for their participation in the study and all members of the Sickle Cell Disease Center from Robert Debré Hospital for the management of blood samples. We thank Dr Marie-Hélène Odièvre for her contribution to patient's recruitment. We are indebted to Wassim El Nemer for helpful comments and for reading the manuscript. This work was supported by a grant from l'Association Recherche et Transfusion, the Institut National de la Transfusion Sanguine, and the Laboratory of Excellence GR-Ex, reference ANR-11-LABX-0051; GR-Ex is funded by the program "Investissements d'avenir" of the French National Research Agency, reference ANR-11-IDEX-0005-02. The Orbitrap Fusion mass spectrometer was acquired with funds from the FEDER through the "Operational Programme for Competitiveness and Employment 2007-2013" and from the "Cancerpole Ile de France".

References

1. Kaul DK, Finnegan E, Barabino GA. Sickle red cell-endothelium interactions. *Microcirculation*. 2009;16(1):97-111.

2. Proenca-Ferreira R, Brugnerotto AF, Garrido VT, et al. Endothelial activation by platelets from sickle cell anemia patients. *PLoS One*. 2014;9(2):e89012.
3. Koehl B, Nivoit P, El Nemer W, et al. The endothelin B receptor plays a crucial role in the adhesion of neutrophils to the endothelium in sickle cell disease. *Haematologica*. 2017;102(7):1161-1172.
4. Platt OS, Brambilla DJ, Rosse WF, et al. Mortality in sickle cell disease. Life expectancy and risk factors for early death. *N Engl J Med*. 1994;330(23):1639-1644.
5. Lum AF, Wun T, Staunton D, Simon SI. Inflammatory potential of neutrophils detected in sickle cell disease. *Am J Hematol*. 2004;76(2):126-133.
6. Yang P, Li Y, Xie Y, Liu Y. Different Faces for Different Places: Heterogeneity of Neutrophil Phenotype and Function. *J Immunol Res*. 2019;2019:8016254.
7. Wang X, Qiu L, Li Z, Wang XY, Yi H. Understanding the Multifaceted Role of Neutrophils in Cancer and Autoimmune Diseases. *Front Immunol*. 2018;9:2456.
8. Zhang D, Xu C, Manwani D, Frenette PS. Neutrophils, platelets, and inflammatory pathways at the nexus of sickle cell disease pathophysiology. *Blood*. 2016;127(7):801-809.
9. Geiger T, Wehner A, Schaab C, Cox J, Mann M. Comparative proteomic analysis of eleven common cell lines reveals ubiquitous but varying expression of most proteins. *Mol Cell Proteomics*. 2012;11(3):M111.014050.
10. Fadlon E, Vordermeier S, Pearson TC, et al. Blood polymorphonuclear leukocytes from the majority of sickle cell patients in the crisis phase of the disease show enhanced adhesion to vascular endothelium and increased expression of CD64. *Blood*. 1998;91(1):266-274.
11. Bancerek J, Poss ZC, Steinparzer I, et al. CDK8 kinase phosphorylates transcription factor STAT1 to selectively regulate the interferon response. *Immunity*. 2013;38(2):250-262.

12. Wiesauer I, Gaumannmuller C, Steinparzer I, Strobl B, Kovarik P. Promoter occupancy of STAT1 in interferon responses is regulated by processive transcription. *Mol Cell Biol.* 2015;35(4):716-727.
13. Crow MK, Ronnblom L. Type I interferons in host defence and inflammatory diseases. *Lupus Sci Med.* 2019;6(1):e000336.
14. Liu D, Gibb DR, Escamilla-Rivera V, et al. Type 1 IFN signaling critically regulates influenza-induced alloimmunization to transfused KEL RBCs in a murine model. *Transfusion.* 2019;59(10):3243-3252.
15. Gibb DR, Liu J, Natarajan P, et al. Type I IFN Is Necessary and Sufficient for Inflammation-Induced Red Blood Cell Alloimmunization in Mice. *J Immunol.* 2017;199(3):1041-1050.

Figure Legends

Figure 1: Proteomic analysis of neutrophils from healthy donors (AA) and SS patients (SS) at steady state. **A.** Overall proteomics results: number of proteins identified and quantified in at least one sample (A) or in at least 3 samples and in at least one group (B). **B.** 2D enrichment analysis of the proteins expressed in at least 75% of the samples and in at least one group. Protein annotation databases from GOBP. Annotations out of the diagonal corresponding to differential expression in SS or AA samples are indicated. **C.** Cluster analysis of proteins differentially expressed in SS and AA neutrophils. Proteins with significantly different expression values (p value < 0.05 and fold change > 0.3) were selected, their LFQ values were z score transformed and analyzed by Euclidian clustering. Clusters 1 and 2 correspond to proteins upregulated and downregulated in SS neutrophils, respectively. **D.** Cluster analysis of differentially expressed proteins with the “cellular response to type I interferon” GOBP annotation. **E.** Characterization of neutrophils from SS patients by flow cytometry analysis, typical result: over-expression of Fc fragment of IgG/CD64 and under-expression of L-selectin/CD62L. Data are presented as mean \pm SD. Mann-Whitney test was used to compare SS and AA; *, $p < 0.05$ compared with AA; **, $p < 0.01$ compared with AA.

Figure 2: Activation of IFN-1 pathway in SS neutrophils. **A.** Representative images of western blots for MX1, IFIT-1, ISG15, STAT 1, Phospho-STAT 1, STAT 2 and Phospho-STAT 2 expressed in neutrophils from healthy volunteers (AA, $n=10$) and SS patients (SS, $n=10$). The western blots are represented as the ratio of the density of the specific band on the total protein in each sample. **B.** Level of IFN α and IFN β in plasma from healthy donors (AA, $n=34$) and SS patients at basal state (SS, $n=37$) using a digital-ELISA assay (SIMOA). **C.** Level of Neutrophil elastase and nucleosome in plasma from healthy Donors (AA, $n=12$) and SS patients at basal state (SS, $n=28$) using ELISA assay. Data are presented as mean \pm SD. Mann-Whitney test was used to compare SS and AA; *, $p < 0.05$ compared with AA; **, $p < 0.01$ compared with AA; ***, $p < 0.001$.

Figure 1

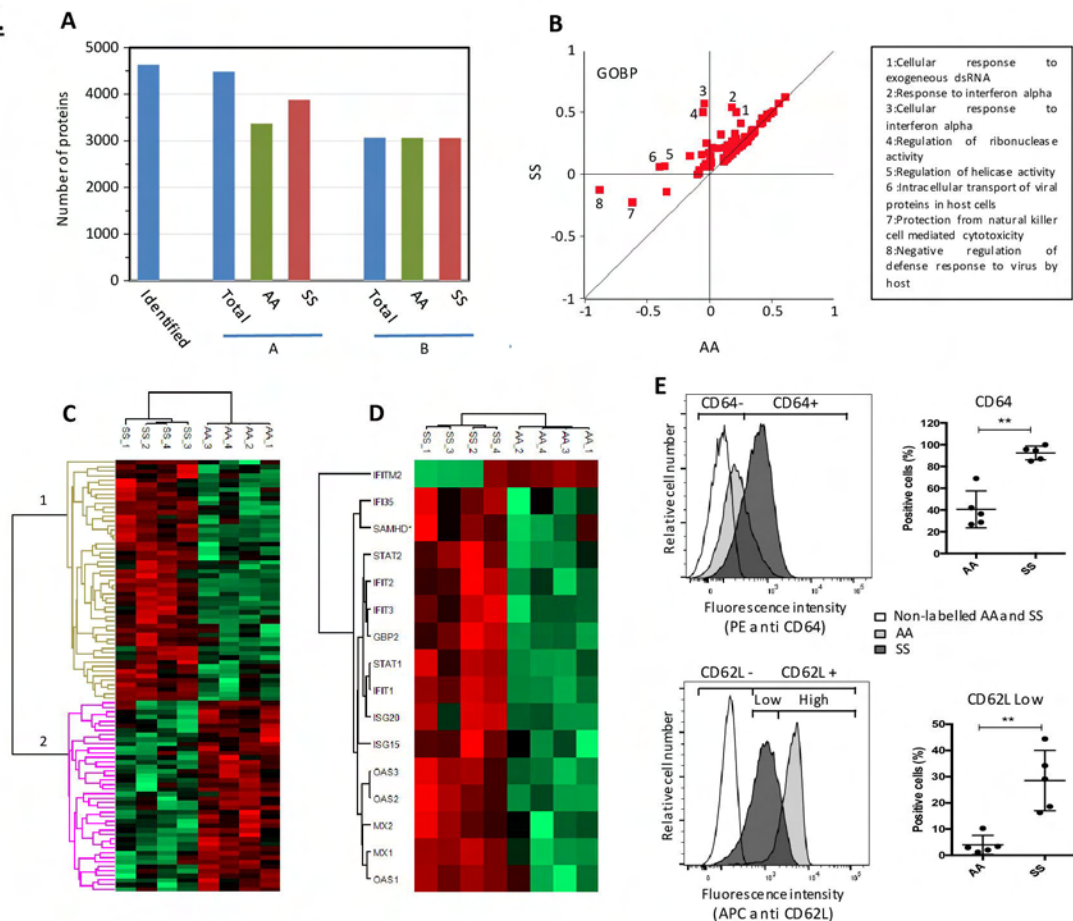
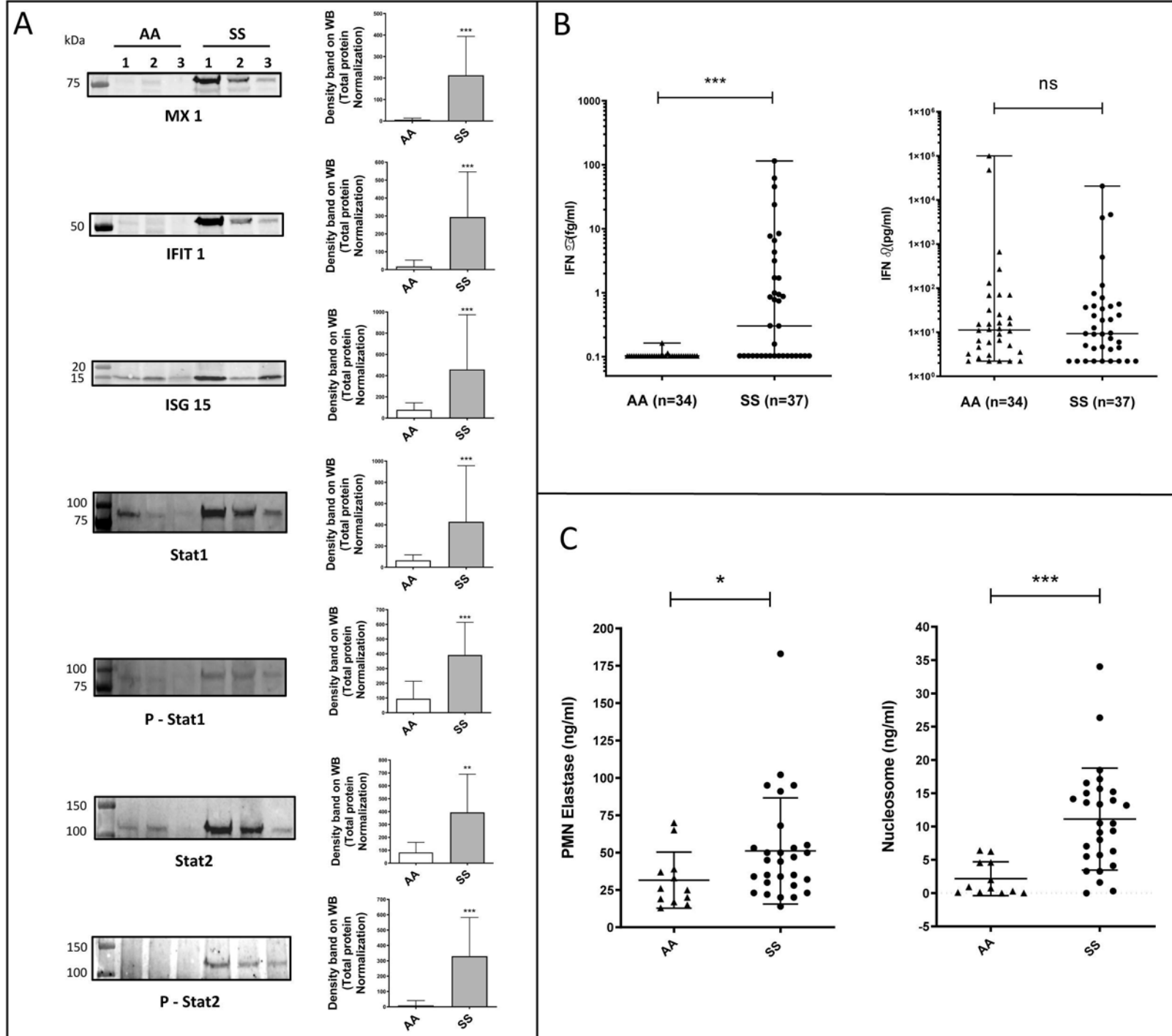


Figure 2



Supplementary Methods

Patients and healthy volunteers

Blood samples were collected on ethylenediamine tetraacetic acid (EDTA) from patients with sickle cell anemia (SS genotype), and from healthy donors (Etablissement Français du Sang). SS patients were children aged 2 to 18 years old, at steady state (no concomitant infection, no acute events in the last month and no blood transfusion within the last 3 months, not treated with hydroxycarbamide. Blood samples used in this study were recovered from blood tubes drawn for medical care, in accordance with French legislation. The study was approved by the French Ethical Committee (CPP 74/18_3). Biological characteristics of the patients included in the study are summarized in Supplementary Table 2.

Human neutrophil isolation

Human neutrophils were isolated as previously described ⁴, using Neutrophil Isolation Kit followed by MACSxpress Erythrocyte Depletion Kit MACSxpress (Miltenyi Biotec, Paris France). The protocol of neutrophil purification was optimized by monitoring two parameters: the CD16 labelling by flow cytometry and the presence of contaminant proteins from RBCs (hemoglobin), platelets (CD41) and lymphocytes (CD3 and CD19). As shown in the proteomic file, none of these proteins was detected in the neutrophils from control and SS patients. In addition, flow cytometry analysis showed that more than 99 % of these cells were CD16-positive.

Label free quantification analysis

Purified PMNs were incubated at 4°C for 5 minutes in 1 mL PBS containing 2mM Diisopropylfluorophosphate (Sigma) to avoid excessive protein degradation during sample preparation. After three washes in cold PBS, 2×10^6 neutrophils were lysed and sonicated in 100

μl Tris/HCl 100 mM pH8.5, SDS 2%, 1mM PMSF. Then, 50μg of proteins were reduced with 10 mM TCEP, alkylated with 40 mM chloroacetamide and digested with 1 μg trypsin using the FASP protocol ¹. Peptides were separated in 5 fractions by strong cationic exchange (SCX) StageTips ² and analyzed using an Orbitrap Fusion mass spectrometer (Thermo Scientific). Peptides from each SCX fraction were separated on a C18 reverse phase column (2μm particle size, 100 Å pore size, 75μm inner diameter, 25cm length) with a 3hr gradient starting from 99% of solvent A containing 0.1% formic acid, ending in 40% of solvent B containing 80% ACN and 0.085% formic acid. The MS1 scans spanned from 350-1500 m/z with 1.10⁶ Automated Gain Control (AGC) target, within 60ms maximum ion injection time (MIIT) and a resolution set to 60,000. In a 3 seconds window, as many Higher energy Collisional Dissociation (HCD) fragmentations as possible were performed on the most abundant ions and subsequently measured in the ion trap (data-dependent acquisition with top speed mode: 3 seconds cycle) with a dynamic exclusion time of 30s. Precursor selection window was set at 1.6 m/z with quadrupole filtering. HCD Normalized Collision Energy was set at 30% and the ion trap scan rate was set to “rapid” mode with AGC target 1.10⁵ and 60ms MIIT. The mass spectrometry data were analyzed using Maxquant (v.1.6.1.0) ³. The database used was a concatenation of human sequences from the Uniprot-Swissprot database (release 2017-05) and the list of contaminant sequences from Maxquant. Cystein carbamidomethylation was set as constant modification and acetylation of protein N-terminus and oxidation of methionine were set as variable modifications. Second peptide search and the “match between runs” (MBR) options were allowed. Label-free protein quantification (LFQ) was done using both unique and razor peptides with at least 2 such peptides required for LFQ. Statistical analysis and data comparison were done using the Perseus software version 1.6.2.3 (Sup Table S1)⁴. The mass spectrometry proteomics data have been deposited to the ProteomeXchange Consortium via the PRIDE partner repository with the dataset identifier PXD014457.

Flow Cytometry

Expression of CD62L and CD64 on purified neutrophils was tested with APC Anti-Human CD62L Antibody (Biolegend – clone DREG-56) and PE Anti-Human CD64 Antibody (Biolegend – clone 10.1).

Western Blot Analysis

Purified neutrophils were lysed in lysis buffer containing 100 mM Tris/HCl (pH8.5), SDS 2%, 1mM PMSF, Phosphatase Inhibitor Cocktail 3 (Sigma - ref P0044), complete EDTA-free (Roche – ref 11 873 580 001). The total protein concentration was determined by the BCA method (Pierce, Thermo Fisher Scientific) and 50 µg of proteins were separated by 4 - 15% SDS– PAGE using TGX Stain-Free Precast Gel (Bio-Rad) under reducing conditions. The gel was imaged using the stain-free application on the ChemiDoc MP (Bio-Rad) imager immediately after the protein separation in order to normalize the loading charge (Figure Sup 1). Blots were probed with anti-Human MX1 (HPA030917 – Sigma 0,4µg/ml), anti-Human IFIT1 (PA3-848 – ThermoFisher Scientific 1:2000), anti-Human ISG15 (MAB 4845 - R&D System 0,5µg/ml), anti-Human Stat 1 (clone 10C4B40 – Biolegend 1µg/ml), anti-Human Stat2 (MAB1666 – R&D Systems 0,2µg/ml), anti-Human Phospho-Stat1 (MAB2894- R&D Systems 0,25µg/ml) and anti-Human Phospho-Stat2 (AF2890 – R&D Systems 0,5µg/ml). Immune complexes were revealed with secondary peroxidase-conjugated antibodies (Abliance) using a chemiluminescent kit (Clarity Western ECL Substrate - Bio-Rad).

Quantification of Interferon alpha and beta at the protein level in plasma

Whole blood was collected from SS patients at steady state and after centrifugation at 5 mn at 3000 rpm, plasma was collected and frozen at -20°C. Interferon alpha (IFNα) and Interferon beta (IFNβ) protein level was quantified using a digital-ELISA assay (SIMOA, Quanterix) developed by Roderio et al ⁵ for the first dosage and the UMR INSERM 1223 (Institut Pasteur)

for the second. For IFN α quantification, the 8H1 antibody clone was used as a capture antibody, after coating on paramagnetic beads (0.3 mg/ml), and the 12H5 antibody was biotinylated (biotin-to-antibody ratio 30: 1) and used as the detector. Detector and revelation enzyme SBG concentrations were 0,3 ug/mL and 150 pM respectively. For IFN β quantification, a mouse anti-human IFN β Antibody (PBL Assay Science, Cat No. 710322-9), was used as a capture antibody, after coating on paramagnetic beads (0.3 mg/ml), and a mouse anti-human IFN β Antibody (PBL Assay Science, Cat. No. 710323-9) was biotinylated (biotin-to-antibody ratio 40: 1) and used as the detector. Detector and revelation enzyme SBG concentrations were 1 ug/mL and 50 pM respectively. Recombinant IFN α 17/ α I (PBL Assay Science) and IFN β (PBL Assay Science) were used to generate a standard curve, after cross-reactivity testing. Each plasma sample was analyzed in duplicate and in dilution 1:6. The limit of detection (LOD) was calculated as the logarithmic mean value +2SD (95% confidence) of reactivity from all blank runs, and found to be 0.10 fg/mL for IFN α and 2.2 pg/mL for IFN β , including the dilution factor.

PMN elastase and nucleosome detection

The PMN Elastase and Nucleosome plasma levels were detected using PMN Elastase Human Elisa Kit (ab119553 Abcam) and NU.QTM H3.1 Assay Kit (ACTIVE MOTIF) respectively.

References

1. Gautier EF, Ducamp S, Leduc M, et al. Comprehensive Proteomic Analysis of Human Erythropoiesis. *Cell Rep.* 2016;16(5):1470-1484.
2. Kulak NA, Pichler G, Paron I, Nagaraj N, Mann M. Minimal, encapsulated proteomic-sample processing applied to copy-number estimation in eukaryotic cells. *Nat Methods.* 2014;11(3):319-324.

3. Cox JT, Marginean I, Kelly RT, Smith RD, Tang K. Improving the sensitivity of mass spectrometry by using a new sheath flow electrospray emitter array at subambient pressures. *J Am Soc Mass Spectrom.* 2014;25(12):2028-2037.
4. Koehl B, Nivoit P, El Nemer W, et al. The endothelin B receptor plays a crucial role in the adhesion of neutrophils to the endothelium in sickle cell disease. *Haematologica.* 2017;102(7):1161-72.
5. Rodero MP, Decalf J, Bondet V, et al. Detection of interferon alpha protein reveals differential levels and cellular sources in disease. *J Exp Med.* 2017;214(5):1547-1555.

Supplementary Figure

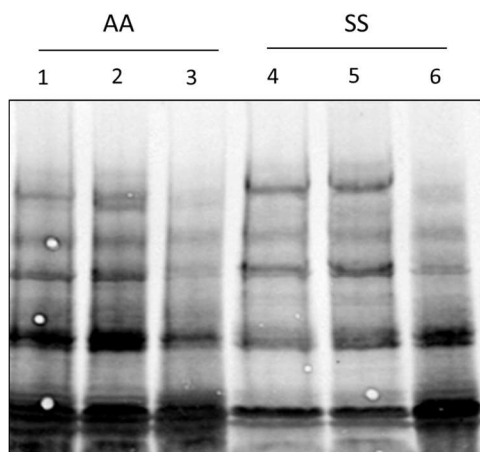


Figure 1: Representative image of stain free gel after proteins migration (Total protein quantification).

Supplementary Tables

Table S1: Proteins differentially expressed in neutrophils from sickle cell patients (SS) vs healthy controls (AA).

| Majority protein IDs | Protein names | Gene names | AA_1 | AA_2 | AA_3 | AA_4 | SS_1 | SS_2 | SS_3 | SS_4 | Mean AA | Mean SS | -Log Student's T-test p-value SS_AA | Student's T-test Difference SS_AA | SS/AA |
|----------------------|--|------------|---------|---------|---------|---------|---------|---------|---------|---------|---------|---------|-------------------------------------|-----------------------------------|---------|
| P09914 | IFN-induced protein with tetra-ricopeptide repeats 1 | IFIT1 | 17,6306 | 17,0796 | 16,2158 | 16,9758 | 23,1873 | 24,6123 | 21,9317 | 23,7321 | 16,9755 | 23,3659 | 4,2645 | 6,3904 | 83,8890 |
| P29728 | 2-5-oligoadenylate synthase 2 | OAS2 | 17,0016 | 17,2935 | 17,0214 | 18,2788 | 23,2258 | 21,1454 | 22,0749 | 20,3726 | 17,3988 | 21,7047 | 3,1238 | 4,3058 | 19,7782 |
| Q460N5 | Poly [ADP-ribose] polymerase 14 | PARP14 | 18,2098 | 17,7407 | 17,8754 | 17,7234 | 21,5247 | 21,8790 | 21,4010 | 22,7942 | 17,8873 | 21,8997 | 4,6917 | 4,0124 | 16,1384 |
| Q9Y6K5 | 2-5-oligoadenylate synthase 3 | OAS3 | 18,1771 | 18,7753 | 17,4432 | 18,4351 | 23,2829 | 22,3736 | 22,1773 | 20,9838 | 18,2077 | 22,2044 | 3,4578 | 3,9967 | 15,9638 |
| P09913 | IFN-induced protein with tetra-ricopeptide repeats 2 | IFIT2 | 19,7427 | 19,1782 | 18,0975 | 20,3704 | 21,9375 | 24,9266 | 22,1713 | 23,9141 | 19,3472 | 23,2374 | 2,3911 | 3,8902 | 14,8270 |
| Q96PP8 | Guanylate-binding protein 5 | GBP5 | 16,4967 | 18,0774 | 16,6524 | 17,0859 | 19,0098 | 22,8031 | 19,3429 | 22,4778 | 17,0781 | 20,9084 | 1,9415 | 3,8303 | 14,2242 |
| P20591 | IFN-induced GTP-binding protein Mx1 | MX1 | 20,4169 | 21,6133 | 20,3094 | 19,6485 | 24,0278 | 24,3996 | 23,8484 | 23,5453 | 20,4970 | 23,9553 | 3,6149 | 3,4583 | 10,9911 |
| P00973 | 2-5-oligoadenylate synthase 1 | OAS1 | 17,0946 | 19,1196 | 15,5582 | 16,4074 | 20,3866 | 20,2646 | 19,7027 | 19,8545 | 17,0450 | 20,0521 | 2,0832 | 3,0072 | 8,0398 |
| P05161 | Ubiquitin-like protein ISG15 | ISG15 | 18,0213 | 20,8144 | 20,0177 | 19,2291 | 21,8059 | 23,9405 | 21,7090 | 22,0424 | 19,5206 | 22,3745 | 1,9392 | 2,8538 | 7,2291 |
| Q07617 | Sperm-associated antigen 1 | SPAG1 | 17,6151 | 17,0886 | 16,9808 | 16,2487 | 16,6035 | 20,3178 | 21,2198 | 20,7903 | 16,9833 | 19,7329 | 1,3374 | 2,7496 | 6,7252 |
| P12314 | High affinity Ig gamma Fc receptor I/II | FCGR1A/B | 17,2710 | 16,2445 | 16,8662 | 18,8060 | 19,7422 | 19,9231 | 20,2469 | 19,4608 | 17,2969 | 19,8433 | 2,3721 | 2,5463 | 5,8414 |
| O14879 | IFN-induced protein with tetra-ricopeptide repeats 3 | IFIT3 | 21,4377 | 20,2648 | 21,5279 | 21,5148 | 23,2633 | 24,2520 | 22,7124 | 24,5943 | 21,1863 | 23,7055 | 2,4904 | 2,5192 | 5,7325 |
| Q8TDB6 | E3 ubiquitin-protein ligase DTX3L | DTX3L | 19,6162 | 20,2100 | 19,6638 | 16,6017 | 21,4904 | 21,4646 | 21,2188 | 21,0403 | 19,0229 | 21,3035 | 1,4855 | 2,2806 | 4,8588 |
| Q8NI27 | THO complex subunit 2 | THOC2 | 16,3739 | 15,9833 | 17,6767 | 17,8081 | 19,0663 | 18,9885 | 19,0285 | 19,2648 | 16,9605 | 19,0870 | 2,4282 | 2,1265 | 4,3666 |
| Q08380 | Galectin-3-binding protein | LGALS3BP | 19,0167 | 18,4537 | 17,0446 | 17,2786 | 21,1594 | 20,1928 | 20,1977 | 18,6709 | 17,9484 | 20,0552 | 1,6313 | 2,1068 | 4,3073 |
| P32456 | IFN-induced guanylate-binding protein 2 | GBP2 | 19,4783 | 19,5362 | 19,9056 | 19,8705 | 21,0230 | 22,4414 | 21,4366 | 22,0795 | 19,6977 | 21,7451 | 3,0463 | 2,0475 | 4,1337 |
| Q9Y3Z3 | Deoxynucleoside 3-phosphate 3-phosphohydrolase SAMHD1 | SAMHD1 | 22,8509 | 20,3389 | 21,3191 | 20,7537 | 24,5717 | 23,3856 | 22,3239 | 22,8817 | 21,3157 | 23,2907 | 1,4540 | 1,9751 | 3,9316 |
| O95497 | Pantetheinase | VNN1 | 24,8357 | 21,4171 | 24,2315 | 22,8256 | 24,8228 | 25,3776 | 25,4256 | 25,4481 | 23,3275 | 25,2685 | 1,3296 | 1,9411 | 3,8399 |
| A6N173 | Leukocyte Ig-like receptor subfamily A member 5 | LILRA5 | 17,1800 | 19,2376 | 19,8396 | 18,0182 | 20,0378 | 20,5703 | 19,7991 | 20,9649 | 18,5689 | 20,3430 | 1,4579 | 1,7742 | 3,4204 |
| P52630 | Signal transducer and activator of transcription 2 | STAT2 | 18,6623 | 17,5919 | 17,9983 | 17,9429 | 19,3084 | 20,5262 | 19,8268 | 19,6039 | 18,0489 | 19,8163 | 2,6804 | 1,7675 | 3,4045 |
| Q6PCE3 | Glucose 1,6-bisphosphate synthase | PGM2L1 | 16,6097 | 18,2502 | 19,2094 | 17,3670 | 19,6927 | 19,4237 | 19,3695 | 19,4010 | 17,8591 | 19,4717 | 1,5341 | 1,6127 | 3,0582 |
| Q96A26 | IFN-stimulated gene 20 kDa protein | ISG20 | 19,5721 | 19,9045 | 19,5719 | 19,9634 | 21,5689 | 21,8406 | 20,1762 | 21,7132 | 19,7530 | 21,3247 | 2,1082 | 1,5718 | 2,9727 |
| P20592 | IFN-induced GTP-binding protein Mx2 | MX2 | 21,5514 | 22,0098 | 21,4505 | 20,3502 | 23,5309 | 22,6182 | 23,0196 | 22,3945 | 21,3405 | 22,8908 | 1,9416 | 1,5503 | 2,9288 |
| P16083 | Ribosyl-dihydroxynicotinamide dehydrogenase [quinone] | NQO2 | 23,3081 | 24,3284 | 22,6231 | 23,9042 | 24,2649 | 25,0914 | 24,9914 | 25,5506 | 23,5410 | 24,9746 | 1,6987 | 1,4336 | 2,7012 |
| P48449 | Lanosterol synthase | LSS | 17,2169 | 17,3683 | 17,4552 | 16,2695 | 18,1367 | 18,5761 | 19,4852 | 17,6722 | 17,0775 | 18,4676 | 1,5840 | 1,3901 | 2,6209 |
| P42285 | Superkiller viralicidic activity 2-like 2 | SKIV2L2 | 19,0474 | 20,0253 | 18,7661 | 20,1490 | 20,4782 | 20,6032 | 21,5389 | 20,3166 | 19,4970 | 20,7342 | 1,5057 | 1,2373 | 2,3576 |
| Q96CD2 | Phosphopantothenoyl-cysteine decarboxylase | PPCDC | 17,1574 | 17,5528 | 16,3109 | 17,1211 | 18,3835 | 17,5339 | 19,1364 | 17,9563 | 17,0356 | 18,2525 | 1,5241 | 1,2170 | 2,3246 |
| P42224 | Signal transducer and activator of transcription 1-alpha/beta | STAT1 | 23,0540 | 22,8181 | 22,7244 | 22,7409 | 24,2764 | 24,1472 | 23,5606 | 24,0584 | 22,8344 | 24,0107 | 3,2909 | 1,1763 | 2,2599 |
| Q9H0P0 | Cytosolic 5-nucleotidase 3A | NT5C3A | 19,3011 | 19,5023 | 18,8220 | 20,4082 | 21,2020 | 20,5248 | 20,3318 | 20,2887 | 19,5084 | 20,5868 | 1,4714 | 1,0784 | 2,1117 |
| P15848 | Arylsulfatase B | ARSB | 21,1209 | 20,2354 | 20,0379 | 20,1193 | 21,1441 | 22,1369 | 21,1852 | 21,3507 | 20,3784 | 21,4542 | 1,7028 | 1,0758 | 2,1079 |
| A6N1G2 | Ankyrin repeat domain-containing protein SOWAHD | SOWAHD | 19,6336 | 18,8184 | 18,3546 | 19,3581 | 20,6143 | 19,9196 | 19,8691 | 19,9175 | 19,0412 | 20,0801 | 1,6712 | 1,0390 | 2,0548 |
| P28838 | Cytosol aminopeptidase | LAP3 | 21,8149 | 21,9839 | 21,8469 | 22,2432 | 23,6003 | 22,6126 | 22,3526 | 23,0350 | 21,9722 | 22,9001 | 1,7340 | 0,9279 | 1,9025 |
| Q8IXQ6 | Poly [ADP-ribose] polymerase 9 | PARP9 | 19,4319 | 19,2454 | 18,9366 | 19,8998 | 20,9426 | 20,3751 | 20,3135 | 19,5816 | 19,3784 | 20,3032 | 1,4408 | 0,9248 | 1,8984 |
| Q9NX24 | H/ACA ribonucleoprotein complex subunit 2 | NHP2 | 17,3472 | 17,4200 | 17,6330 | 17,1373 | 18,3210 | 18,8741 | 17,5471 | 18,2572 | 17,3844 | 18,2499 | 1,6069 | 0,8655 | 1,8220 |
| Q63HN8 | E3 ubiquitin-protein ligase RNF213 | RNF213 | 21,9781 | 22,3333 | 21,6712 | 22,5042 | 22,9591 | 23,2448 | 22,8147 | 22,9209 | 22,1217 | 22,9849 | 2,2275 | 0,8632 | 1,8191 |
| Q92785 | Zinc finger protein ubi-d4 | DPF2 | 19,0827 | 19,0579 | 19,4253 | 19,0896 | 19,3996 | 19,8862 | 20,3189 | 20,3410 | 19,1639 | 19,9864 | 1,8652 | 0,8226 | 1,7686 |
| P80217 | IFN-induced 35 kDa protein | IFI35 | 23,1715 | 22,4880 | 22,8614 | 23,3483 | 24,0913 | 23,6633 | 23,3746 | 23,8804 | 22,9673 | 23,7524 | 1,7461 | 0,7851 | 1,7232 |
| P46013 | Antigen KI-67 | MKI67 | 18,1513 | 18,0456 | 18,2313 | 18,5656 | 19,6379 | 19,2215 | 18,4460 | 18,7612 | 18,2485 | 19,0167 | 1,4498 | 0,7682 | 1,7032 |
| Q6P2E9 | Enhancer of mRNA-decapping protein 4 | EDC4 | 19,0396 | 19,1500 | 19,2026 | 19,1664 | 19,9614 | 19,7695 | 20,0358 | 19,4576 | 19,1397 | 19,8061 | 2,6038 | 0,6664 | 1,5871 |
| Q9NUV9 | GTPase IMAF family member 4 | GIMAP4 | 21,7343 | 21,7545 | 21,8816 | 22,4917 | 22,4324 | 22,2917 | 23,1985 | 22,6003 | 21,9655 | 22,6307 | 1,3238 | 0,6652 | 1,5858 |
| Q43598 | 2-deoxynucleoside 5-phosphate N-hydrolase 1 | DNPH1 | 19,4574 | 19,8877 | 19,5328 | 19,1317 | 20,2842 | 20,2606 | 20,2689 | 19,8539 | 19,5024 | 20,1669 | 1,9200 | 0,6645 | 1,5851 |
| Q9BR76 | Coronin-18 | CORO18 | 22,1507 | 22,2846 | 21,2500 | 21,9179 | 22,3456 | 22,6384 | 22,6212 | 22,6177 | 21,9008 | 22,5557 | 1,4638 | 0,6549 | 1,5746 |
| Q9Y3L3 | SH3 domain-binding protein 1 | SH3BP1 | 23,1940 | 23,3158 | 23,9196 | 23,1087 | 24,0122 | 24,4172 | 23,8051 | 23,8773 | 23,3845 | 24,0280 | 1,5141 | 0,6434 | 1,5620 |
| Q03518 | Antigen peptide transporter 1 | TAP1 | 21,7705 | 21,9095 | 22,3633 | 22,0024 | 22,4884 | 22,9625 | 22,4802 | 22,6023 | 22,0114 | 22,6334 | 1,9765 | 0,6219 | 1,5389 |
| P42167 | Lamina-associated polypeptide 2, isoforms beta/gamma; Thymopoietin;Thymopentin | TMPO | 22,3040 | 22,1904 | 22,2848 | 22,1096 | 22,4091 | 23,0824 | 22,5674 | 23,2431 | 22,2222 | 22,8255 | 1,5869 | 0,6033 | 1,5192 |
| Q8IY16 | Exocyst complex component 8 | EXOC8 | 19,6101 | 19,8119 | 19,7653 | 19,7945 | 20,6187 | 20,2871 | 20,3841 | 20,0985 | 19,7455 | 20,3471 | 2,6597 | 0,6017 | 1,5175 |
| Q9UIA0 | Cytohesin-4 | CYTH4 | 20,1987 | 19,7985 | 20,3568 | 20,3370 | 20,3266 | 21,1542 | 20,6627 | 20,9468 | 20,1728 | 20,7726 | 1,4537 | 0,5998 | 1,5155 |
| Q96IJ7 | Protein disulfide-isomerase TMX3 | TMX3 | 19,6739 | 19,9195 | 20,1740 | 20,4406 | 20,2616 | 21,0468 | 20,4993 | 20,7268 | 20,0520 | 20,6336 | 1,3180 | 0,5816 | 1,4965 |
| Q04637 | Eukaryotic translation initiation factor 4 gamma 1 | EIF4G1 | 20,5581 | 20,4764 | 19,7668 | 20,3719 | 20,9488 | 21,0840 | 20,5460 | 20,8940 | 20,2933 | 20,8682 | 1,4482 | 0,5749 | 1,4896 |
| Q92541 | RNA polymerase-associated protein RTF1 | RTF1 | 19,4723 | 19,5159 | 20,0776 | 19,9366 | 20,3481 | 20,4028 | 20,4338 | 20,1172 | 19,7506 | 20,3255 | 1,8587 | 0,5749 | 1,4895 |
| O60934 | Nibrin | NBN | 17,9139 | 17,8160 | 17,0775 | 17,2489 | 17,9672 | 18,3550 | 18,1033 | 17,8950 | 17,5141 | 18,0801 | 1,3092 | 0,5661 | 1,4805 |
| P05023 | Na/K-transporting ATPase unit alpha-1 | ATP1A1 | 23,4059 | 23,8402 | 23,4151 | 23,2076 | 24,1507 | 24,3707 | 23,7792 | 23,7288 | 23,4672 | 24,0074 | 1,4251 | 0,5401 | 1,4541 |
| P08567 | Pleckstrin | PLEK | 23,4596 | 23,7550 | 23,8458 | 23,9921 | 23,8524 | 24,3516 | 24,4987 | 24,4370 | 23,7631 | 24,2849 | 1,5160 | 0,5218 | 1,4358 |

| | | | | | | | | | | | | | | | |
|---------------|--|------------|---------|---------|---------|---------|---------|---------|---------|---------|---------|---------|--------|---------|---------------|
| P19525 | IFN-induced, double-stranded RNA-activated protein kinase | EIF2AK2 | 22,4310 | 22,5569 | 22,6624 | 22,4481 | 23,1477 | 22,9944 | 22,5877 | 23,3365 | 22,5246 | 23,0166 | 1,5796 | 0,4920 | 1,4064 |
| Q8NCW5 | NAD(P)H-hydrate epimerase | APOA1BP | 20,7163 | 20,5159 | 20,2400 | 20,3264 | 21,3158 | 21,0813 | 20,7928 | 20,5720 | 20,4497 | 20,9405 | 1,3478 | 0,4908 | 1,4052 |
| P42126 | Enoyl-CoA delta isomerase 1, mitochondrial | EC11 | 21,6078 | 21,6212 | 21,5396 | 21,6420 | 22,0819 | 22,2968 | 22,3479 | 21,6121 | 21,6027 | 22,0847 | 1,5342 | 0,4820 | 1,3967 |
| Q8TDK7 | Serine/threonine-protein kinase Nek7 | NEK7 | 20,7621 | 20,4995 | 20,8100 | 20,5702 | 21,1515 | 20,9028 | 21,3124 | 21,2002 | 20,6605 | 21,1417 | 2,2523 | 0,4813 | 1,3960 |
| Q9NPB8 | Glycerophosphocholine phosphodiesterase GPCPD1 | GPCPD1 | 20,0784 | 19,6634 | 19,6284 | 19,5776 | 20,1679 | 20,2976 | 20,4210 | 19,9862 | 19,7370 | 20,2182 | 1,7584 | 0,4812 | 1,3959 |
| Q9NR97 | Toll-like receptor 8 | TLR8 | 20,3349 | 20,2876 | 20,2932 | 20,4138 | 21,0846 | 20,7608 | 20,7704 | 20,6136 | 20,3324 | 20,8074 | 2,4314 | 0,4750 | 1,3899 |
| P55209 | Nucleosome assembly protein 1-like 1 | NAP1L1 | 21,9212 | 21,4764 | 21,6816 | 21,2179 | 22,0545 | 22,3426 | 22,0106 | 21,7647 | 21,5743 | 22,0431 | 1,3071 | 0,4688 | 1,3840 |
| P23396 | 40S ribosomal protein S3 | RPS3 | 24,0071 | 24,2700 | 24,2966 | 23,8426 | 24,4695 | 24,8311 | 24,4755 | 24,5083 | 24,1041 | 24,5711 | 1,8114 | 0,4671 | 1,3823 |
| Q9GZ53 | WD repeat-containing protein 61 | WDR61 | 21,1732 | 20,9455 | 20,4310 | 20,6475 | 21,3702 | 21,1992 | 21,2836 | 21,0752 | 20,7993 | 21,2321 | 1,3167 | 0,4327 | 1,3498 |
| P19971 | Thymidine phosphorylase | TYMP | 23,8723 | 24,2279 | 24,4978 | 24,2447 | 24,9407 | 24,4187 | 24,6463 | 24,5299 | 24,2107 | 24,6339 | 1,3199 | 0,4233 | 1,3410 |
| O75170 | Ser/thr-protein phosphatase 6 regulatory subunit 2 | PPP6R2 | 17,8641 | 17,9931 | 18,2165 | 17,8105 | 18,6599 | 18,0862 | 18,5889 | 18,2010 | 17,9711 | 18,3840 | 1,3086 | 0,4130 | 1,3314 |
| P61081 | NEDD8-conjugating enzyme Ubc12 | UBE2M | 21,8932 | 21,8126 | 21,6235 | 22,1170 | 22,3110 | 22,2843 | 22,2014 | 22,2918 | 21,8616 | 22,2721 | 2,1024 | 0,4106 | 1,3292 |
| Q16836 | Hydroxyacyl-coenzyme A dehydrogenase, mitochondrial | HADH | 22,1748 | 22,4674 | 22,5930 | 22,2766 | 22,9039 | 23,0349 | 22,6637 | 22,4941 | 22,3780 | 22,7742 | 1,3839 | 0,3962 | 1,3160 |
| P08708 | 40S ribosomal protein S17 | RPS17 | 22,1169 | 22,7520 | 22,4054 | 22,4855 | 22,9683 | 22,8794 | 22,8060 | 22,6492 | 22,4400 | 22,8257 | 1,4035 | 0,3858 | 1,3066 |
| Q13547 | Histone deacetylase 1 | HDAC1 | 21,9185 | 21,7085 | 21,4312 | 21,5484 | 22,0138 | 22,2064 | 22,0788 | 21,8407 | 21,6517 | 22,0349 | 1,5888 | 0,3833 | 1,3043 |
| Q8IZP0 | Abl interactor 1 | ABI1 | 22,8213 | 22,9518 | 23,0852 | 22,9010 | 22,6273 | 22,3108 | 22,4705 | 22,2168 | 22,9398 | 22,4064 | 2,6250 | -0,5335 | 0,6909 |
| Q8N6G5 | Chondroitin sulfate N-acetylgalactosaminyltransferase 2 | CSGALNACT2 | 19,7296 | 20,2416 | 20,0701 | 20,0868 | 19,4466 | 19,8439 | 19,7060 | 18,9834 | 20,0320 | 19,4950 | 1,3110 | -0,5371 | 0,6892 |
| Q9H4E7 | Differentially expressed in FDCP 6 homolog | DEF6 | 24,8964 | 25,0351 | 24,8873 | 24,6704 | 24,4424 | 24,4761 | 24,0352 | 24,3445 | 24,8723 | 24,3246 | 2,3234 | -0,5478 | 0,6841 |
| Q9BS26 | Endoplasmic reticulum resident prot 44 | ERP44 | 23,8473 | 23,6431 | 23,9407 | 23,4472 | 23,3476 | 23,3960 | 23,2108 | 22,7029 | 23,7196 | 23,1643 | 1,5491 | -0,5553 | 0,6805 |
| Q9UHQ9 | NADH-cytochrome b5 reductase 1 | CYB5R1 | 20,7390 | 21,2354 | 21,1577 | 21,0397 | 20,7409 | 20,5658 | 20,2656 | 20,3228 | 21,0430 | 20,4738 | 1,9810 | -0,5692 | 0,6740 |
| Q9UL26 | Ras-related protein Rab-22A | RAB22A | 20,5266 | 20,6231 | 19,9243 | 20,5573 | 19,5694 | 20,0395 | 20,0140 | 19,6594 | 20,4078 | 19,8206 | 1,5650 | -0,5872 | 0,6656 |
| P16035 | Metalloproteinase inhibitor 2 | TIMP2 | 21,9818 | 22,3032 | 22,8198 | 22,5434 | 22,0193 | 21,7909 | 21,8805 | 21,5728 | 22,4121 | 21,8159 | 1,5990 | -0,5962 | 0,6615 |
| Q8TD16 | Protein bicaudal D homolog 2 | BICD2 | 21,5524 | 21,1111 | 21,0929 | 21,0624 | 21,0548 | 20,8723 | 20,1368 | 20,3025 | 21,2047 | 20,5916 | 1,3081 | -0,6131 | 0,6538 |
| P51531 | Probable global transcription activator SNF2L2 | SMARCA2 | 21,6360 | 21,5468 | 21,5106 | 21,2147 | 21,0025 | 20,6291 | 21,2804 | 20,4937 | 21,4770 | 20,8514 | 1,6830 | -0,6256 | 0,6482 |
| Q8IWB1 | Inositol 1,4,5-trisphosphate receptor-interacting protein | ITPRIP | 22,4264 | 22,2500 | 22,7764 | 21,9612 | 21,6123 | 21,8092 | 21,9834 | 21,4464 | 22,3535 | 21,7128 | 1,6758 | -0,6407 | 0,6414 |
| Q9H9C1 | Spermatogenesis-defective protein 39 homolog | VIPAS39 | 18,8040 | 18,6583 | 18,8868 | 18,7271 | 17,8680 | 18,1415 | 18,6365 | 17,8650 | 18,7691 | 18,1278 | 1,8437 | -0,6413 | 0,6411 |
| P14151 | L-selectin | SELL | 22,4399 | 22,1500 | 22,5939 | 23,1440 | 22,1385 | 21,8365 | 21,5070 | 22,1769 | 22,5820 | 21,9147 | 1,3687 | -0,6673 | 0,6297 |
| B01172 | Unconventional myosin-Ig;Minor histocompatibility Ag HA-2 | MYO1G | 24,5158 | 24,7384 | 24,7477 | 24,6020 | 23,9951 | 23,5076 | 24,1826 | 24,2383 | 24,6510 | 23,9809 | 2,0587 | -0,6701 | 0,6285 |
| Q96F46 | Interleukin-17 receptor A | IL17RA | 19,7837 | 19,2913 | 19,7885 | 19,3368 | 19,1617 | 18,6373 | 18,5727 | 19,0527 | 19,5501 | 18,8561 | 1,8681 | -0,6940 | 0,6181 |
| Q13231 | Chitotriosidase-1 | CHIT1 | 25,9270 | 26,2744 | 26,4691 | 26,1441 | 24,9679 | 25,8165 | 25,4025 | 25,6878 | 26,2037 | 25,4687 | 1,8085 | -0,7350 | 0,6008 |
| Q9NX63 | MICOS complex subunit MIC19 | CHCHD3 | 21,3488 | 21,1412 | 21,5205 | 21,3281 | 20,9324 | 20,8734 | 20,1521 | 20,3876 | 21,3347 | 20,5864 | 1,9739 | -0,7482 | 0,5953 |
| P36969 | Phospholipid hydroperoxide glutathione peroxidase, mitochondrial | GPX4 | 21,1484 | 21,7407 | 21,2892 | 22,0126 | 21,0726 | 20,2065 | 21,0936 | 20,7592 | 21,5477 | 20,7830 | 1,4249 | -0,7647 | 0,5886 |
| O15269 | Serine palmitoyltransferase 1 | SPTLC1 | 19,3018 | 19,8295 | 19,7621 | 20,2439 | 19,1124 | 18,5471 | 19,5232 | 18,6315 | 19,7843 | 18,9536 | 1,4996 | -0,8308 | 0,5622 |
| Q9Y6D9 | Mitotic spindle assembly checkpoint protein MAD1 | MAD1L1 | 18,4612 | 18,6761 | 18,9210 | 18,9878 | 17,4297 | 18,1385 | 18,3257 | 17,7621 | 18,7615 | 17,9140 | 1,9636 | -0,8475 | 0,5557 |
| P54803 | Galactocerebrosidase | GALC | 20,7814 | 19,9461 | 19,6193 | 19,6413 | 19,0791 | 18,9975 | 19,3598 | 19,0906 | 19,9970 | 19,1318 | 1,6513 | -0,8653 | 0,5489 |
| P02766 | Transthyretin | TTR | 20,6680 | 21,5788 | 21,4412 | 20,8077 | 20,0284 | 20,5664 | 20,0756 | 20,2534 | 21,1239 | 20,2310 | 1,8772 | -0,8930 | 0,5385 |
| P02647 | Apolipoprotein A-I;Proapolipoprotein A-I | APOA1 | 24,0277 | 23,7420 | 24,0567 | 23,9971 | 22,5193 | 23,7640 | 22,6651 | 23,1110 | 23,9559 | 23,0149 | 1,7623 | -0,9411 | 0,5208 |
| P19484 | Transcription factor EB | TFEB | 19,6419 | 20,4104 | 19,9601 | 20,1108 | 19,4729 | 18,2499 | 19,0317 | 19,2418 | 20,0308 | 18,9991 | 1,8008 | -1,0318 | 0,4891 |
| P61313 | 60S ribosomal protein L15 | RPL15 | 20,2370 | 19,5332 | 20,2734 | 19,6657 | 17,7118 | 19,3875 | 19,0635 | 18,9136 | 19,9273 | 18,7691 | 1,5087 | -1,1583 | 0,4481 |
| Q148N4 | Sarcolemmal membrane-associated protein | SLMAP | 19,8176 | 20,2104 | 19,8138 | 20,7223 | 18,9587 | 18,4436 | 18,4837 | 19,2567 | 20,1410 | 18,7857 | 2,4607 | -1,3554 | 0,3908 |
| Q53FT3 | Protein Hikeshi | C11orf73 | 20,1191 | 20,8815 | 20,2166 | 20,9114 | 20,6166 | 18,2176 | 18,4650 | 19,0190 | 20,5322 | 19,0796 | 1,3375 | -1,4526 | 0,3654 |
| Q8N1B4 | Vacuolar protein sorting-associated protein 52 homolog | VP52 | 18,9368 | 20,0679 | 19,2876 | 20,1531 | 18,4672 | 18,9580 | 17,6187 | 17,2739 | 19,6114 | 18,0795 | 1,7009 | -1,5319 | 0,3458 |
| P61244 | Protein max | MAX | 20,2986 | 20,9458 | 20,0359 | 20,0058 | 18,9281 | 17,2074 | 18,8988 | 20,0637 | 20,3215 | 18,7745 | 1,3114 | -1,5470 | 0,3422 |
| P01008 | Antithrombin-III | SERPINC1 | 18,2219 | 20,3870 | 19,1727 | 18,5176 | 17,7143 | 17,2942 | 17,3212 | 17,0635 | 19,0748 | 17,3483 | 1,8706 | -1,7265 | 0,3022 |
| Q99627 | COP9 signalosome complex subunit 8 | COPS8 | 19,1007 | 18,5057 | 18,8823 | 18,8904 | 19,1331 | 16,3659 | 16,0797 | 16,8084 | 18,8448 | 17,0968 | 1,3180 | -1,7480 | 0,2977 |
| Q9HCC0 | Methylcrotonoyl-CoA carboxylase beta chain, mitochondrial | MCCC2 | 19,4584 | 18,3582 | 17,7548 | 18,5053 | 17,0523 | 15,8861 | 16,8560 | 17,1724 | 18,5192 | 16,7417 | 2,0872 | -1,7775 | 0,2917 |
| Q9UNL2 | Translocon-associated protein subunit gamma | SSR3 | 17,4809 | 18,8660 | 19,9545 | 18,9434 | 17,6980 | 16,7075 | 16,2196 | 15,7090 | 18,8112 | 16,5835 | 1,8212 | -2,2277 | 0,2135 |
| Q01629 | IFN-induced transmembrane protein 2 | IFITM2 | 24,2082 | 23,8126 | 25,0992 | 24,3506 | 16,1419 | 16,5493 | 16,3932 | 24,8603 | 24,3677 | 18,4862 | 1,4743 | -5,8815 | 0,0170 |

Table S2: Hematological parameters of SS patients with low and high IFN α levels

| | Low IFN α level (<0.12 fg/mL) (n=17) | High IFN α level (>0.12 fg/mL) (n=20) | <i>P</i> |
|---|--|---|----------|
| Age (years) | 10.28 [4.55-14.48] | 9.19 [4.07-14.31] | 0.53 |
| Hb level (g/dl) | 8.84 [7.67-10.01] | 8.24 [7.26-9.22] | 0.33 |
| Leucocyte count (/mm³) | 14,700 [7,400-22,000] | 11,300 [7,600-15,000] | 0.15 |
| Platelet count (/mm³) | 360,700 [176,400-545,000] | 263,700 [91,300-436,000] | 0.55 |
| Neutrophil count (/mm³) | 5,970 [3,990-8,940] | 5,750 [4,090-7,400] | 0.82 |
| Reticulocyte count (/mm³) | 297,370 [157,820-436,930] | 258,100 [186,800-329,300] | 0.53 |

Supplementary Methods

Patients and healthy volunteers

Blood samples were collected on ethylenediamine tetraacetic acid (EDTA) from patients with sickle cell anemia (SS genotype), and from healthy donors (Etablissement Français du Sang). SS patients were children aged 2 to 18 years old, at steady state (no concomitant infection, no acute events in the last month and no blood transfusion within the last 3 months, not treated with hydroxycarbamide. Blood samples used in this study were recovered from blood tubes drawn for medical care, in accordance with French legislation. The study was approved by the French Ethical Committee (CPP 74/18_3). Biological characteristics of the patients included in the study are summarized in Supplementary Table 2.

Human neutrophil isolation

Human neutrophils were isolated as previously described ⁴, using Neutrophil Isolation Kit followed by MACSxpress Erythrocyte Depletion Kit MACSxpress (Miltenyi Biotec, Paris France). The protocol of neutrophil purification was optimized by monitoring two parameters: the CD16 labelling by flow cytometry and the presence of contaminant proteins from RBCs (hemoglobin), platelets (CD41) and lymphocytes (CD3 and CD19). As shown in the proteomic file, none of these proteins was detected in the neutrophils from control and SS patients. In addition, flow cytometry analysis showed that more than 99 % of these cells were CD16-positive.

Label free quantification analysis

Purified PMNs were incubated at 4°C for 5 minutes in 1 mL PBS containing 2mM Diisopropylfluorophosphate (Sigma) to avoid excessive protein degradation during sample preparation. After three washes in cold PBS, 2×10^6 neutrophils were lysed and sonicated in 100

μl Tris/HCl 100 mM pH8.5, SDS 2%, 1mM PMSF. Then, 50μg of proteins were reduced with 10 mM TCEP, alkylated with 40 mM chloroacetamide and digested with 1 μg trypsin using the FASP protocol ¹. Peptides were separated in 5 fractions by strong cationic exchange (SCX) StageTips ² and analyzed using an Orbitrap Fusion mass spectrometer (Thermo Scientific). Peptides from each SCX fraction were separated on a C18 reverse phase column (2μm particle size, 100 Å pore size, 75μm inner diameter, 25cm length) with a 3hr gradient starting from 99% of solvent A containing 0.1% formic acid, ending in 40% of solvent B containing 80% ACN and 0.085% formic acid. The MS1 scans spanned from 350-1500 m/z with 1.10⁶ Automated Gain Control (AGC) target, within 60ms maximum ion injection time (MIIT) and a resolution set to 60,000. In a 3 seconds window, as many Higher energy Collisional Dissociation (HCD) fragmentations as possible were performed on the most abundant ions and subsequently measured in the ion trap (data-dependent acquisition with top speed mode: 3 seconds cycle) with a dynamic exclusion time of 30s. Precursor selection window was set at 1.6 m/z with quadrupole filtering. HCD Normalized Collision Energy was set at 30% and the ion trap scan rate was set to “rapid” mode with AGC target 1.10⁵ and 60ms MIIT. The mass spectrometry data were analyzed using Maxquant (v.1.6.1.0) ³. The database used was a concatenation of human sequences from the Uniprot-Swissprot database (release 2017-05) and the list of contaminant sequences from Maxquant. Cystein carbamidomethylation was set as constant modification and acetylation of protein N-terminus and oxidation of methionine were set as variable modifications. Second peptide search and the “match between runs” (MBR) options were allowed. Label-free protein quantification (LFQ) was done using both unique and razor peptides with at least 2 such peptides required for LFQ. Statistical analysis and data comparison were done using the Perseus software version 1.6.2.3 (Sup Table S1)⁴. The mass spectrometry proteomics data have been deposited to the ProteomeXchange Consortium via the PRIDE partner repository with the dataset identifier PXD014457.

Flow Cytometry

Expression of CD62L and CD64 on purified neutrophils was tested with APC Anti-Human CD62L Antibody (Biolegend – clone DREG-56) and PE Anti-Human CD64 Antibody (Biolegend – clone 10.1).

Western Blot Analysis

Purified neutrophils were lysed in lysis buffer containing 100 mM Tris/HCl (pH8.5), SDS 2%, 1mM PMSF, Phosphatase Inhibitor Cocktail 3 (Sigma - ref P0044), complete EDTA-free (Roche – ref 11 873 580 001). The total protein concentration was determined by the BCA method (Pierce, Thermo Fisher Scientific) and 50 µg of proteins were separated by 4 - 15% SDS– PAGE using TGX Stain-Free Precast Gel (Bio-Rad) under reducing conditions. The gel was imaged using the stain-free application on the ChemiDoc MP (Bio-Rad) imager immediately after the protein separation in order to normalize the loading charge (Figure Sup 1). Blots were probed with anti-Human MX1 (HPA030917 – Sigma 0,4µg/ml), anti-Human IFIT1 (PA3-848 – ThermoFisher Scientific 1:2000), anti-Human ISG15 (MAB 4845 - R&D System 0,5µg/ml), anti-Human Stat 1 (clone 10C4B40 – Biolegend 1µg/ml), anti-Human Stat2 (MAB1666 – R&D Systems 0,2µg/ml), anti-Human Phospho-Stat1 (MAB2894- R&D Systems 0,25µg/ml) and anti-Human Phospho-Stat2 (AF2890 – R&D Systems 0,5µg/ml). Immune complexes were revealed with secondary peroxidase-conjugated antibodies (Abliance) using a chemiluminescent kit (Clarity Western ECL Substrate - Bio-Rad).

Quantification of Interferon alpha and beta at the protein level in plasma

Whole blood was collected from SS patients at steady state and after centrifugation at 5 mn at 3000 rpm, plasma was collected and frozen at -20°C. Interferon alpha (IFNα) and Interferon beta (IFNβ) protein level was quantified using a digital-ELISA assay (SIMOA, Quanterix) developed by Rodero et al ⁵ for the first dosage and the UMR INSERM 1223 (Institut Pasteur)

for the second. For IFN α quantification, the 8H1 antibody clone was used as a capture antibody, after coating on paramagnetic beads (0.3 mg/ml), and the 12H5 antibody was biotinylated (biotin-to-antibody ratio 30: 1) and used as the detector. Detector and revelation enzyme SBG concentrations were 0,3 ug/mL and 150 pM respectively. For IFN β quantification, a mouse anti-human IFN β Antibody (PBL Assay Science, Cat No. 710322-9), was used as a capture antibody, after coating on paramagnetic beads (0.3 mg/ml), and a mouse anti-human IFN β Antibody (PBL Assay Science, Cat. No. 710323-9) was biotinylated (biotin-to-antibody ratio 40: 1) and used as the detector. Detector and revelation enzyme SBG concentrations were 1 ug/mL and 50 pM respectively. Recombinant IFN α 17/ α I (PBL Assay Science) and IFN β (PBL Assay Science) were used to generate a standard curve, after cross-reactivity testing. Each plasma sample was analyzed in duplicate and in dilution 1:6. The limit of detection (LOD) was calculated as the logarithmic mean value +2SD (95% confidence) of reactivity from all blank runs, and found to be 0.10 fg/mL for IFN α and 2.2 pg/mL for IFN β , including the dilution factor.

PMN elastase and nucleosome detection

The PMN Elastase and Nucleosome plasma levels were detected using PMN Elastase Human Elisa Kit (ab119553 Abcam) and NU.QTM H3.1 Assay Kit (ACTIVE MOTIF) respectively.

References

1. Gautier EF, Ducamp S, Leduc M, et al. Comprehensive Proteomic Analysis of Human Erythropoiesis. *Cell Rep.* 2016;16(5):1470-1484.
2. Kulak NA, Pichler G, Paron I, Nagaraj N, Mann M. Minimal, encapsulated proteomic-sample processing applied to copy-number estimation in eukaryotic cells. *Nat Methods.* 2014;11(3):319-324.

3. Cox JT, Marginean I, Kelly RT, Smith RD, Tang K. Improving the sensitivity of mass spectrometry by using a new sheath flow electrospray emitter array at subambient pressures. *J Am Soc Mass Spectrom.* 2014;25(12):2028-2037.
4. Koehl B, Nivoit P, El Nemer W, et al. The endothelin B receptor plays a crucial role in the adhesion of neutrophils to the endothelium in sickle cell disease. *Haematologica.* 2017;102(7):1161-72.
5. Rodero MP, Decalf J, Bondet V, et al. Detection of interferon alpha protein reveals differential levels and cellular sources in disease. *J Exp Med.* 2017;214(5):1547-1555.

Supplementary Figure

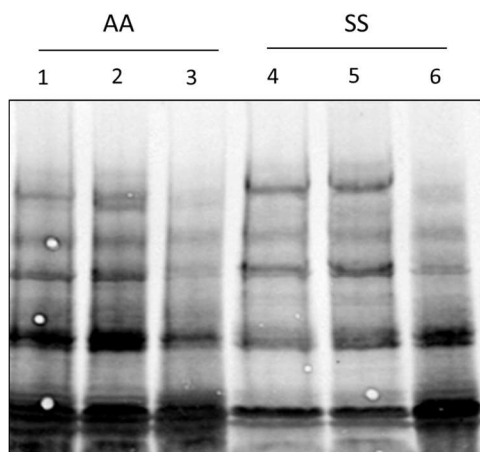


Figure 1: Representative image of stain free gel after proteins migration (Total protein quantification).

Supplementary Tables

Table S1: Proteins differentially expressed in neutrophils from sickle cell patients (SS) vs healthy controls (AA).

| Majority protein IDs | Protein names | Gene names | AA_1 | AA_2 | AA_3 | AA_4 | SS_1 | SS_2 | SS_3 | SS_4 | Mean AA | Mean SS | -Log Student's T-test p-value SS_AA | Student's T-test Difference SS_AA | SS/AA |
|----------------------|--|------------|---------|---------|---------|---------|---------|---------|---------|---------|---------|---------|-------------------------------------|-----------------------------------|---------|
| P09914 | IFN-induced protein with tetra-ricopeptide repeats 1 | IFIT1 | 17,6306 | 17,0796 | 16,2158 | 16,9758 | 23,1873 | 24,6123 | 21,9317 | 23,7321 | 16,9755 | 23,3659 | 4,2645 | 6,3904 | 83,8890 |
| P29728 | 2-5-oligoadenylate synthase 2 | OAS2 | 17,0016 | 17,2935 | 17,0214 | 18,2788 | 23,2258 | 21,1454 | 22,0749 | 20,3726 | 17,3988 | 21,7047 | 3,1238 | 4,3058 | 19,7782 |
| Q460N5 | Poly [ADP-ribose] polymerase 14 | PARP14 | 18,2098 | 17,7407 | 17,8754 | 17,7234 | 21,5247 | 21,8790 | 21,4010 | 22,7942 | 17,8873 | 21,8997 | 4,6917 | 4,0124 | 16,1384 |
| Q9Y6K5 | 2-5-oligoadenylate synthase 3 | OAS3 | 18,1771 | 18,7753 | 17,4432 | 18,4351 | 23,2829 | 22,3736 | 22,1773 | 20,9838 | 18,2077 | 22,2044 | 3,4578 | 3,9967 | 15,9638 |
| P09913 | IFN-induced protein with tetra-ricopeptide repeats 2 | IFIT2 | 19,7427 | 19,1782 | 18,0975 | 20,3704 | 21,9375 | 24,9266 | 22,1713 | 23,9141 | 19,3472 | 23,2374 | 2,3911 | 3,8902 | 14,8270 |
| Q96PP8 | Guanylate-binding protein 5 | GBP5 | 16,4967 | 18,0774 | 16,6524 | 17,0859 | 19,0098 | 22,8031 | 19,3429 | 22,4778 | 17,0781 | 20,9084 | 1,9415 | 3,8303 | 14,2242 |
| P20591 | IFN-induced GTP-binding protein Mx1 | MX1 | 20,4169 | 21,6133 | 20,3094 | 19,6485 | 24,0278 | 24,3996 | 23,8484 | 23,5453 | 20,4970 | 23,9553 | 3,6149 | 3,4583 | 10,9911 |
| P00973 | 2-5-oligoadenylate synthase 1 | OAS1 | 17,0946 | 19,1196 | 15,5582 | 16,4074 | 20,3866 | 20,2646 | 19,7027 | 19,8545 | 17,0450 | 20,0521 | 2,0832 | 3,0072 | 8,0398 |
| P05161 | Ubiquitin-like protein ISG15 | ISG15 | 18,0213 | 20,8144 | 20,0177 | 19,2291 | 21,8059 | 23,9405 | 21,7090 | 22,0424 | 19,5206 | 22,3745 | 1,9392 | 2,8538 | 7,2291 |
| Q07617 | Sperm-associated antigen 1 | SPAG1 | 17,6151 | 17,0886 | 16,9808 | 16,2487 | 16,6035 | 20,3178 | 21,2198 | 20,7903 | 16,9833 | 19,7329 | 1,3374 | 2,7496 | 6,7252 |
| P12314 | High affinity Ig gamma Fc receptor I/II | FCGR1A/B | 17,2710 | 16,2445 | 16,8662 | 18,8060 | 19,7422 | 19,9231 | 20,2469 | 19,4608 | 17,2969 | 19,8433 | 2,3721 | 2,5463 | 5,8414 |
| O14879 | IFN-induced protein with tetra-ricopeptide repeats 3 | IFIT3 | 21,4377 | 20,2648 | 21,5279 | 21,5148 | 23,2633 | 24,2520 | 22,7124 | 24,5943 | 21,1863 | 23,7055 | 2,4904 | 2,5192 | 5,7325 |
| Q8TDB6 | E3 ubiquitin-protein ligase DTX3L | DTX3L | 19,6162 | 20,2100 | 19,6638 | 16,6017 | 21,4904 | 21,4646 | 21,2188 | 21,0403 | 19,0229 | 21,3035 | 1,4855 | 2,2806 | 4,8588 |
| Q8NI27 | THO complex subunit 2 | THOC2 | 16,3739 | 15,9833 | 17,6767 | 17,8081 | 19,0663 | 18,9885 | 19,0285 | 19,2648 | 16,9605 | 19,0870 | 2,4282 | 2,1265 | 4,3666 |
| Q08380 | Galectin-3-binding protein | LGALS3BP | 19,0167 | 18,4537 | 17,0446 | 17,2786 | 21,1594 | 20,1928 | 20,1977 | 18,6709 | 17,9484 | 20,0552 | 1,6313 | 2,1068 | 4,3073 |
| P32456 | IFN-induced guanylate-binding protein 2 | GBP2 | 19,4783 | 19,5362 | 19,9056 | 19,8705 | 21,0230 | 22,4414 | 21,4366 | 22,0795 | 19,6977 | 21,7451 | 3,0463 | 2,0475 | 4,1337 |
| Q9Y3Z3 | Deoxynucleoside 3-phosphate 3-phosphohydrolase SAMHD1 | SAMHD1 | 22,8509 | 20,3389 | 21,3191 | 20,7537 | 24,5717 | 23,3856 | 22,3239 | 22,8817 | 21,3157 | 23,2907 | 1,4540 | 1,9751 | 3,9316 |
| O95497 | Pantetheinase | VNN1 | 24,8357 | 21,4171 | 24,2315 | 22,8256 | 24,8228 | 25,3776 | 25,4256 | 25,4481 | 23,3275 | 25,2685 | 1,3296 | 1,9411 | 3,8399 |
| A6N173 | Leukocyte Ig-like receptor subfamily A member 5 | LILRA5 | 17,1800 | 19,2376 | 19,8396 | 18,0182 | 20,0378 | 20,5703 | 19,7991 | 20,9649 | 18,5689 | 20,3430 | 1,4579 | 1,7742 | 3,4204 |
| P52630 | Signal transducer and activator of transcription 2 | STAT2 | 18,6623 | 17,5919 | 17,9983 | 17,9429 | 19,3084 | 20,5262 | 19,8268 | 19,6039 | 18,0489 | 19,8163 | 2,6804 | 1,7675 | 3,4045 |
| Q6PCE3 | Glucose 1,6-bisphosphate synthase | PGM2L1 | 16,6097 | 18,2502 | 19,2094 | 17,3670 | 19,6927 | 19,4237 | 19,3695 | 19,4010 | 17,8591 | 19,4717 | 1,5341 | 1,6127 | 3,0582 |
| Q96A26 | IFN-stimulated gene 20 kDa protein | ISG20 | 19,5721 | 19,9045 | 19,5719 | 19,9634 | 21,5689 | 21,8406 | 20,1762 | 21,7132 | 19,7530 | 21,3247 | 2,1082 | 1,5718 | 2,9727 |
| P20592 | IFN-induced GTP-binding protein Mx2 | MX2 | 21,5514 | 22,0098 | 21,4505 | 20,3502 | 23,5309 | 22,6182 | 23,0196 | 22,3945 | 21,3405 | 22,8908 | 1,9416 | 1,5503 | 2,9288 |
| P16083 | Ribosyl-dihydroxynicotinamide dehydrogenase [quinone] | NQO2 | 23,3081 | 24,3284 | 22,6231 | 23,9042 | 24,2649 | 25,0914 | 24,9914 | 25,5506 | 23,5410 | 24,9746 | 1,6987 | 1,4336 | 2,7012 |
| P48449 | Lanosterol synthase | LSS | 17,2169 | 17,3683 | 17,4552 | 16,2695 | 18,1367 | 18,5761 | 19,4852 | 17,6722 | 17,0775 | 18,4676 | 1,5840 | 1,3901 | 2,6209 |
| P42285 | Superkiller viralicidic activity 2-like 2 | SKIV2L2 | 19,0474 | 20,0253 | 18,7661 | 20,1490 | 20,4782 | 20,6032 | 21,5389 | 20,3166 | 19,4970 | 20,7342 | 1,5057 | 1,2373 | 2,3576 |
| Q96CD2 | Phosphopantothenoicysteine decarboxylase | PPCDC | 17,1574 | 17,5528 | 16,3109 | 17,1211 | 18,3835 | 17,5339 | 19,1364 | 17,9563 | 17,0356 | 18,2525 | 1,5241 | 1,2170 | 2,3246 |
| P42224 | Signal transducer and activator of transcription 1-alpha/beta | STAT1 | 23,0540 | 22,8181 | 22,7244 | 22,7409 | 24,2764 | 24,1472 | 23,5606 | 24,0584 | 22,8344 | 24,0107 | 3,2909 | 1,1763 | 2,2599 |
| Q9H0P0 | Cytosolic 5-nucleotidase 3A | NT5C3A | 19,3011 | 19,5023 | 18,8220 | 20,4082 | 21,2020 | 20,5248 | 20,3318 | 20,2887 | 19,5084 | 20,5868 | 1,4714 | 1,0784 | 2,1117 |
| P15848 | Arylsulfatase B | ARSB | 21,1209 | 20,2354 | 20,0379 | 20,1193 | 21,1441 | 22,1369 | 21,1852 | 21,3507 | 20,3784 | 21,4542 | 1,7028 | 1,0758 | 2,1079 |
| A6N1G2 | Ankyrin repeat domain-containing protein SOWAHD | SOWAHD | 19,6336 | 18,8184 | 18,3546 | 19,3581 | 20,6143 | 19,9196 | 19,8691 | 19,9175 | 19,0412 | 20,0801 | 1,6712 | 1,0390 | 2,0548 |
| P28838 | Cytosol aminopeptidase | LAP3 | 21,8149 | 21,9839 | 21,8469 | 22,2432 | 23,6003 | 22,6126 | 22,3526 | 23,0350 | 21,9722 | 22,9001 | 1,7340 | 0,9279 | 1,9025 |
| Q8IXQ6 | Poly [ADP-ribose] polymerase 9 | PARP9 | 19,4319 | 19,2454 | 18,9366 | 19,8998 | 20,9426 | 20,3751 | 20,3135 | 19,5816 | 19,3784 | 20,3032 | 1,4408 | 0,9248 | 1,8984 |
| Q9NX24 | H/ACA ribonucleoprotein complex subunit 2 | NHP2 | 17,3472 | 17,4200 | 17,6330 | 17,1373 | 18,3210 | 18,8741 | 17,5471 | 18,2572 | 17,3844 | 18,2499 | 1,6069 | 0,8655 | 1,8220 |
| Q63HN8 | E3 ubiquitin-protein ligase RNF213 | RNF213 | 21,9781 | 22,3333 | 21,6712 | 22,5042 | 22,9591 | 23,2448 | 22,8147 | 22,9209 | 22,1217 | 22,9849 | 2,2275 | 0,8632 | 1,8191 |
| Q92785 | Zinc finger protein ubi-d4 | DPF2 | 19,0827 | 19,0579 | 19,4253 | 19,0896 | 19,3996 | 19,8862 | 20,3189 | 20,3410 | 19,1639 | 19,9864 | 1,8652 | 0,8226 | 1,7686 |
| P80217 | IFN-induced 35 kDa protein | IFI35 | 23,1715 | 22,4880 | 22,8614 | 23,3483 | 24,0913 | 23,6633 | 23,3746 | 23,8804 | 22,9673 | 23,7524 | 1,7461 | 0,7851 | 1,7232 |
| P46013 | Antigen Ki-67 | MKI67 | 18,1513 | 18,0456 | 18,2313 | 18,5656 | 19,6379 | 19,2215 | 18,4460 | 18,7612 | 18,2485 | 19,0167 | 1,4498 | 0,7682 | 1,7032 |
| Q6P2E9 | Enhancer of mRNA-decapping protein 4 | EDC4 | 19,0396 | 19,1500 | 19,2026 | 19,1664 | 19,9614 | 19,7695 | 20,0358 | 19,4576 | 19,1397 | 19,8061 | 2,6038 | 0,6664 | 1,5871 |
| Q9NUV9 | GTPase IMAF family member 4 | GIMAP4 | 21,7343 | 21,7545 | 21,8816 | 22,4917 | 22,4324 | 22,2917 | 23,1985 | 22,6003 | 21,9655 | 22,6307 | 1,3238 | 0,6652 | 1,5858 |
| Q43598 | 2-deoxynucleoside 5-phosphate N-hydrolase 1 | DNPH1 | 19,4574 | 19,8877 | 19,5328 | 19,1317 | 20,2842 | 20,2606 | 20,2689 | 19,8539 | 19,5024 | 20,1669 | 1,9200 | 0,6645 | 1,5851 |
| Q9BR76 | Coronin-18 | CORO18 | 22,1507 | 22,2846 | 21,2500 | 21,9179 | 22,3456 | 22,6384 | 22,6212 | 22,6177 | 21,9008 | 22,5557 | 1,4638 | 0,6549 | 1,5746 |
| Q9Y3L3 | SH3 domain-binding protein 1 | SH3BP1 | 23,1940 | 23,3158 | 23,9196 | 23,1087 | 24,0122 | 24,4172 | 23,8051 | 23,8773 | 23,3845 | 24,0280 | 1,5141 | 0,6434 | 1,5620 |
| Q03518 | Antigen peptide transporter 1 | TAP1 | 21,7705 | 21,9095 | 22,3633 | 22,0024 | 22,4884 | 22,9625 | 22,4802 | 22,6023 | 22,0114 | 22,6334 | 1,9765 | 0,6219 | 1,5389 |
| P42167 | Lamina-associated polypeptide 2, isoforms beta/gamma; Thymopoietin;Thymopentin | TMPO | 22,3040 | 22,1904 | 22,2848 | 22,1096 | 22,4091 | 23,0824 | 22,5674 | 23,2431 | 22,2222 | 22,8255 | 1,5869 | 0,6033 | 1,5192 |
| Q8IY16 | Exocyst complex component 8 | EXOC8 | 19,6101 | 19,8119 | 19,7653 | 19,7945 | 20,6187 | 20,2871 | 20,3841 | 20,0985 | 19,7455 | 20,3471 | 2,6597 | 0,6017 | 1,5175 |
| Q9UIA0 | Cytohesin-4 | CYTH4 | 20,1987 | 19,7985 | 20,3568 | 20,3370 | 20,3266 | 21,1542 | 20,6627 | 20,9468 | 20,1728 | 20,7726 | 1,4537 | 0,5998 | 1,5155 |
| Q96IJ7 | Protein disulfide-isomerase TMX3 | TMX3 | 19,6739 | 19,9195 | 20,1740 | 20,4406 | 20,2616 | 21,0468 | 20,4993 | 20,7268 | 20,0520 | 20,6336 | 1,3180 | 0,5816 | 1,4965 |
| Q04637 | Eukaryotic translation initiation factor 4 gamma 1 | EIF4G1 | 20,5581 | 20,4764 | 19,7668 | 20,3719 | 20,9488 | 21,0840 | 20,5460 | 20,8940 | 20,2933 | 20,8682 | 1,4482 | 0,5749 | 1,4896 |
| Q92541 | RNA polymerase-associated protein RTF1 | RTF1 | 19,4723 | 19,5159 | 20,0776 | 19,9366 | 20,3481 | 20,4028 | 20,4338 | 20,1172 | 19,7506 | 20,3255 | 1,8587 | 0,5749 | 1,4895 |
| O60934 | Nibrin | NBN | 17,9139 | 17,8160 | 17,0775 | 17,2489 | 17,9672 | 18,3550 | 18,1033 | 17,8950 | 17,5141 | 18,0801 | 1,3092 | 0,5661 | 1,4805 |
| P05023 | Na/K-transporting ATPase unit alpha-1 | ATP1A1 | 23,4059 | 23,8402 | 23,4151 | 23,2076 | 24,1507 | 24,3707 | 23,7792 | 23,7288 | 23,4672 | 24,0074 | 1,4251 | 0,5401 | 1,4541 |
| P08567 | Pleckstrin | PLEK | 23,4596 | 23,7550 | 23,8458 | 23,9921 | 23,8524 | 24,3516 | 24,4987 | 24,4370 | 23,7631 | 24,2849 | 1,5160 | 0,5218 | 1,4358 |

| | | | | | | | | | | | | | | | |
|---------------|--|------------|---------|---------|---------|---------|---------|---------|---------|---------|---------|---------|--------|---------|---------------|
| P19525 | IFN-induced, double-stranded RNA-activated protein kinase | EIF2AK2 | 22,4310 | 22,5569 | 22,6624 | 22,4481 | 23,1477 | 22,9944 | 22,5877 | 23,3365 | 22,5246 | 23,0166 | 1,5796 | 0,4920 | 1,4064 |
| Q8NCW5 | NAD(P)H-hydrate epimerase | APOA1BP | 20,7163 | 20,5159 | 20,2400 | 20,3264 | 21,3158 | 21,0813 | 20,7928 | 20,5720 | 20,4497 | 20,9405 | 1,3478 | 0,4908 | 1,4052 |
| P42126 | Enoyl-CoA delta isomerase 1, mitochondrial | EC11 | 21,6078 | 21,6212 | 21,5396 | 21,6420 | 22,0819 | 22,2968 | 22,3479 | 21,6121 | 21,6027 | 22,0847 | 1,5342 | 0,4820 | 1,3967 |
| Q8TDK7 | Serine/threonine-protein kinase Nek7 | NEK7 | 20,7621 | 20,4995 | 20,8100 | 20,5702 | 21,1515 | 20,9028 | 21,3124 | 21,2002 | 20,6605 | 21,1417 | 2,2523 | 0,4813 | 1,3960 |
| Q9NPB8 | Glycerophosphocholine phosphodiesterase GPCPD1 | GPCPD1 | 20,0784 | 19,6634 | 19,6284 | 19,5776 | 20,1679 | 20,2976 | 20,4210 | 19,9862 | 19,7370 | 20,2182 | 1,7584 | 0,4812 | 1,3959 |
| Q9NR97 | Toll-like receptor 8 | TLR8 | 20,3349 | 20,2876 | 20,2932 | 20,4138 | 21,0846 | 20,7608 | 20,7704 | 20,6136 | 20,3324 | 20,8074 | 2,4314 | 0,4750 | 1,3899 |
| P55209 | Nucleosome assembly protein 1-like 1 | NAP1L1 | 21,9212 | 21,4764 | 21,6816 | 21,2179 | 22,0545 | 22,3426 | 22,0106 | 21,7647 | 21,5743 | 22,0431 | 1,3071 | 0,4688 | 1,3840 |
| P23396 | 40S ribosomal protein S3 | RPS3 | 24,0071 | 24,2700 | 24,2966 | 23,8426 | 24,4695 | 24,8311 | 24,4755 | 24,5083 | 24,1041 | 24,5711 | 1,8114 | 0,4671 | 1,3823 |
| Q9GZ53 | WD repeat-containing protein 61 | WDR61 | 21,1732 | 20,9455 | 20,4310 | 20,6475 | 21,3702 | 21,1992 | 21,2836 | 21,0752 | 20,7993 | 21,2321 | 1,3167 | 0,4327 | 1,3498 |
| P19971 | Thymidine phosphorylase | TYMP | 23,8723 | 24,2279 | 24,4978 | 24,2447 | 24,9407 | 24,4187 | 24,6463 | 24,5299 | 24,2107 | 24,6339 | 1,3199 | 0,4233 | 1,3410 |
| O75170 | Ser/thr-protein phosphatase 6 regulatory subunit 2 | PPP6R2 | 17,8641 | 17,9931 | 18,2165 | 17,8105 | 18,6599 | 18,0862 | 18,5889 | 18,2010 | 17,9711 | 18,3840 | 1,3086 | 0,4130 | 1,3314 |
| P61081 | NEDD8-conjugating enzyme Ubc12 | UBE2M | 21,8932 | 21,8126 | 21,6235 | 22,1170 | 22,3110 | 22,2843 | 22,2014 | 22,2918 | 21,8616 | 22,2721 | 2,1024 | 0,4106 | 1,3292 |
| Q16836 | Hydroxyacyl-coenzyme A dehydrogenase, mitochondrial | HADH | 22,1748 | 22,4674 | 22,5930 | 22,2766 | 22,9039 | 23,0349 | 22,6637 | 22,4941 | 22,3780 | 22,7742 | 1,3839 | 0,3962 | 1,3160 |
| P08708 | 40S ribosomal protein S17 | RPS17 | 22,1169 | 22,7520 | 22,4054 | 22,4855 | 22,9683 | 22,8794 | 22,8060 | 22,6492 | 22,4400 | 22,8257 | 1,4035 | 0,3858 | 1,3066 |
| Q13547 | Histone deacetylase 1 | HDAC1 | 21,9185 | 21,7085 | 21,4312 | 21,5484 | 22,0138 | 22,2064 | 22,0788 | 21,8407 | 21,6517 | 22,0349 | 1,5888 | 0,3833 | 1,3043 |
| Q8IZP0 | Abl interactor 1 | ABI1 | 22,8213 | 22,9518 | 23,0852 | 22,9010 | 22,6273 | 22,3108 | 22,4705 | 22,2168 | 22,9398 | 22,4064 | 2,6250 | -0,5335 | 0,6909 |
| Q8N6G5 | Chondroitin sulfate N-acetylgalactosaminyltransferase 2 | CSGALNACT2 | 19,7296 | 20,2416 | 20,0701 | 20,0868 | 19,4466 | 19,8439 | 19,7060 | 18,9834 | 20,0320 | 19,4950 | 1,3110 | -0,5371 | 0,6892 |
| Q9H4E7 | Differentially expressed in FDCP 6 homolog | DEF6 | 24,8964 | 25,0351 | 24,8873 | 24,6704 | 24,4424 | 24,4761 | 24,0352 | 24,3445 | 24,8723 | 24,3246 | 2,3234 | -0,5478 | 0,6841 |
| Q9BS26 | Endoplasmic reticulum resident prot 44 | ERP44 | 23,8473 | 23,6431 | 23,9407 | 23,4472 | 23,3476 | 23,3960 | 23,2108 | 22,7029 | 23,7196 | 23,1643 | 1,5491 | -0,5553 | 0,6805 |
| Q9UHQ9 | NADH-cytochrome b5 reductase 1 | CYB5R1 | 20,7390 | 21,2354 | 21,1577 | 21,0397 | 20,7409 | 20,5658 | 20,2656 | 20,3228 | 21,0430 | 20,4738 | 1,9810 | -0,5692 | 0,6740 |
| Q9UL26 | Ras-related protein Rab-22A | RAB22A | 20,5266 | 20,6231 | 19,9243 | 20,5573 | 19,5694 | 20,0395 | 20,0140 | 19,6594 | 20,4078 | 19,8206 | 1,5650 | -0,5872 | 0,6656 |
| P16035 | Metalloproteinase inhibitor 2 | TIMP2 | 21,9818 | 22,3032 | 22,8198 | 22,5434 | 22,0193 | 21,7909 | 21,8805 | 21,5728 | 22,4121 | 21,8159 | 1,5990 | -0,5962 | 0,6615 |
| Q8TD16 | Protein bicaudal D homolog 2 | BICD2 | 21,5524 | 21,1111 | 21,0929 | 21,0624 | 21,0548 | 20,8723 | 20,1368 | 20,3025 | 21,2047 | 20,5916 | 1,3081 | -0,6131 | 0,6538 |
| P51531 | Probable global transcription activator SNF2L2 | SMARCA2 | 21,6360 | 21,5468 | 21,5106 | 21,2147 | 21,0025 | 20,6291 | 21,2804 | 20,4937 | 21,4770 | 20,8514 | 1,6830 | -0,6256 | 0,6482 |
| Q8IWB1 | Inositol 1,4,5-trisphosphate receptor-interacting protein | ITPRIP | 22,4264 | 22,2500 | 22,7764 | 21,9612 | 21,6123 | 21,8092 | 21,9834 | 21,4464 | 22,3535 | 21,7128 | 1,6758 | -0,6407 | 0,6414 |
| Q9H9C1 | Spermatogenesis-defective protein 39 homolog | VIPAS39 | 18,8040 | 18,6583 | 18,8868 | 18,7271 | 17,8680 | 18,1415 | 18,6365 | 17,8650 | 18,7691 | 18,1278 | 1,8437 | -0,6413 | 0,6411 |
| P14151 | L-selectin | SELL | 22,4399 | 22,1500 | 22,5939 | 23,1440 | 22,1385 | 21,8365 | 21,5070 | 22,1769 | 22,5820 | 21,9147 | 1,3687 | -0,6673 | 0,6297 |
| B01172 | Unconventional myosin-Ig;Minor histocompatibility Ag HA-2 | MYO1G | 24,5158 | 24,7384 | 24,7477 | 24,6020 | 23,9951 | 23,5076 | 24,1826 | 24,2383 | 24,6510 | 23,9809 | 2,0587 | -0,6701 | 0,6285 |
| Q96F46 | Interleukin-17 receptor A | IL17RA | 19,7837 | 19,2913 | 19,7885 | 19,3368 | 19,1617 | 18,6373 | 18,5727 | 19,0527 | 19,5501 | 18,8561 | 1,8681 | -0,6940 | 0,6181 |
| Q13231 | Chitotriosidase-1 | CHIT1 | 25,9270 | 26,2744 | 26,4691 | 26,1441 | 24,9679 | 25,8165 | 25,4025 | 25,6878 | 26,2037 | 25,4687 | 1,8085 | -0,7350 | 0,6008 |
| Q9NX63 | MICOS complex subunit MIC19 | CHCHD3 | 21,3488 | 21,1412 | 21,5205 | 21,3281 | 20,9324 | 20,8734 | 20,1521 | 20,3876 | 21,3347 | 20,5864 | 1,9739 | -0,7482 | 0,5953 |
| P36969 | Phospholipid hydroperoxide glutathione peroxidase, mitochondrial | GPX4 | 21,1484 | 21,7407 | 21,2892 | 22,0126 | 21,0726 | 20,2065 | 21,0936 | 20,7592 | 21,5477 | 20,7830 | 1,4249 | -0,7647 | 0,5886 |
| O15269 | Serine palmitoyltransferase 1 | SPTLC1 | 19,3018 | 19,8295 | 19,7621 | 20,2439 | 19,1124 | 18,5471 | 19,5232 | 18,6315 | 19,7843 | 18,9536 | 1,4996 | -0,8308 | 0,5622 |
| Q9Y6D9 | Mitotic spindle assembly checkpoint protein MAD1 | MAD1L1 | 18,4612 | 18,6761 | 18,9210 | 18,9878 | 17,4297 | 18,1385 | 18,3257 | 17,7621 | 18,7615 | 17,9140 | 1,9636 | -0,8475 | 0,5557 |
| P54803 | Galactocerebrosidase | GALC | 20,7814 | 19,9461 | 19,6193 | 19,6413 | 19,0791 | 18,9975 | 19,3598 | 19,0906 | 19,9970 | 19,1318 | 1,6513 | -0,8653 | 0,5489 |
| P02766 | Transthyretin | TTR | 20,6680 | 21,5788 | 21,4412 | 20,8077 | 20,0284 | 20,5664 | 20,0756 | 20,2534 | 21,1239 | 20,2310 | 1,8772 | -0,8930 | 0,5385 |
| P02647 | Apolipoprotein A-I;Proapolipoprotein A-I | APOA1 | 24,0277 | 23,7420 | 24,0567 | 23,9971 | 22,5193 | 23,7640 | 22,6651 | 23,1110 | 23,9559 | 23,0149 | 1,7623 | -0,9411 | 0,5208 |
| P19484 | Transcription factor EB | TFEB | 19,6419 | 20,4104 | 19,9601 | 20,1108 | 19,4729 | 18,2499 | 19,0317 | 19,2418 | 20,0308 | 18,9991 | 1,8008 | -1,0318 | 0,4891 |
| P61313 | 60S ribosomal protein L15 | RPL15 | 20,2370 | 19,5332 | 20,2734 | 19,6657 | 17,7118 | 19,3875 | 19,0635 | 18,9136 | 19,9273 | 18,7691 | 1,5087 | -1,1583 | 0,4481 |
| Q148N4 | Sarcolemmal membrane-associated protein | SLMAP | 19,8176 | 20,2104 | 19,8138 | 20,7223 | 18,9587 | 18,4436 | 18,4837 | 19,2567 | 20,1410 | 18,7857 | 2,4607 | -1,3554 | 0,3908 |
| Q53FT3 | Protein Hikeshi | C11orf73 | 20,1191 | 20,8815 | 20,2166 | 20,9114 | 20,6166 | 18,2176 | 18,4650 | 19,0190 | 20,5322 | 19,0796 | 1,3375 | -1,4526 | 0,3654 |
| Q8N1B4 | Vacuolar protein sorting-associated protein 52 homolog | VP52 | 18,9368 | 20,0679 | 19,2876 | 20,1531 | 18,4672 | 18,9580 | 17,6187 | 17,2739 | 19,6114 | 18,0795 | 1,7009 | -1,5319 | 0,3458 |
| P61244 | Protein max | MAX | 20,2986 | 20,9458 | 20,0359 | 20,0058 | 18,9281 | 17,2074 | 18,8988 | 20,0637 | 20,3215 | 18,7745 | 1,3114 | -1,5470 | 0,3422 |
| P01008 | Antithrombin-III | SERPINC1 | 18,2219 | 20,3870 | 19,1727 | 18,5176 | 17,7143 | 17,2942 | 17,3212 | 17,0635 | 19,0748 | 17,3483 | 1,8706 | -1,7265 | 0,3022 |
| Q99627 | COP9 signalosome complex subunit 8 | COPS8 | 19,1007 | 18,5057 | 18,8823 | 18,8904 | 19,1331 | 16,3659 | 16,0797 | 16,8084 | 18,8448 | 17,0968 | 1,3180 | -1,7480 | 0,2977 |
| Q9HCC0 | Methylcrotonoyl-CoA carboxylase beta chain, mitochondrial | MCCC2 | 19,4584 | 18,3582 | 17,7548 | 18,5053 | 17,0523 | 15,8861 | 16,8560 | 17,1724 | 18,5192 | 16,7417 | 2,0872 | -1,7775 | 0,2917 |
| Q9UNL2 | Translocon-associated protein subunit gamma | SSR3 | 17,4809 | 18,8660 | 19,9545 | 18,9434 | 17,6980 | 16,7075 | 16,2196 | 15,7090 | 18,8112 | 16,5835 | 1,8212 | -2,2277 | 0,2135 |
| Q01629 | IFN-induced transmembrane protein 2 | IFITM2 | 24,2082 | 23,8126 | 25,0992 | 24,3506 | 16,1419 | 16,5493 | 16,3932 | 24,8603 | 24,3677 | 18,4862 | 1,4743 | -5,8815 | 0,0170 |

Table S2: Hematological parameters of SS patients with low and high IFN α levels

| | Low IFN α level (<0.12 fg/mL) (n=17) | High IFN α level (>0.12 fg/mL) (n=20) | <i>P</i> |
|---|--|---|----------|
| Age (years) | 10.28 [4.55-14.48] | 9.19 [4.07-14.31] | 0.53 |
| Hb level (g/dl) | 8.84 [7.67-10.01] | 8.24 [7.26-9.22] | 0.33 |
| Leucocyte count (/mm³) | 14,700 [7,400-22,000] | 11,300 [7,600-15,000] | 0.15 |
| Platelet count (/mm³) | 360,700 [176,400-545,000] | 263,700 [91,300-436,000] | 0.55 |
| Neutrophil count (/mm³) | 5,970 [3,990-8,940] | 5,750 [4,090-7,400] | 0.82 |
| Reticulocyte count (/mm³) | 297,370 [157,820-436,930] | 258,100 [186,800-329,300] | 0.53 |